DEPARTMENT OF COMMERCE

SCIENTIFIC PAPERS

OF THE

BUREAU OF STANDARDS

GEORGE K. BURGESS, DIRECTOR

VOLUME 19

1923–24

WASHINGTON
GOVERNMENT PRINTING OFFICE
1925

CONTENTS OF VOLUME 19

DEPARTMENT OF COMMERCE
BUREAU OF STANDARDS
George K. Burgess, Director

SCIENTIFIC PAPERS OF THE BUREAU OF STANDARDS, No. 494
[Part of Vol. 19]

ABERRATIONS OF LONG FOCUS ANASTIGMATIC PHOTOGRAPHIC OBJECTIVES

BY

A. H. BENNETT, Associate Physicist
Bureau of Standards

October 16, 1924

PRICE, 20 CENTS
$1.25 PER VOLUME ON SUBSCRIPTION
Sold only by the Superintendent of Documents, Government Printing Office
Washington, D. C.

WASHINGTON
GOVERNMENT PRINTING OFFICE
1924

ABERRATIONS OF LONG FOCUS ANASTIGMATIC PHOTOGRAPHIC OBJECTIVES

By A. H. Bennett

ABSTRACT

No lens system gives perfect definition because of the inherent aberrations of spherical refracting surfaces. The aberrations of a centered lens system are defined, and the characteristic manner in which each aberration affects the image is discussed. Methods for the determination of the various aberrations of a photographic objective are described. The Hartmann method, for which a special camera was designed, was used for the measurement of spherical aberration and departure from the sine condition, while a lens-bench method was employed in the measurement of curvature of field, astigmatism, distortion, and lateral and axial chromatism. The aberrations of 33 photographic objectives of the anastigmatic type, made by different manufacturers, are presented graphically. The variation among individual lenses from the same manufacturer as well as differences found in lenses of the same construction, but by different manufacturers, are discussed.

CONTENTS

I. INTRODUCTION

To place before the public data on the performance of photographic objectives of the anastigmatic type, to indicate to designers what characteristics may be sought in the further development of high-speed photographic lenses, and also to describe methods employed in lens measurements which have been found to be reliable and of requisite precision is the object of this paper.

The lenses investigated were all high-grade anastigmats having aperture ratios ranging from f: 4.5 to f: 7. The long focal lengths of these lenses, from 295 to 1,250 mm, made conditions very favorable for accurate measurements of the aberrations in terms of the focal lengths.

The manufacturers have kindly supplied us with diagrammatic sketches showing the construction of the various types of lenses investigated.

II. ABERRATIONS OF A CENTERED LENS SYSTEM

The presence of errors or aberrations inherent in lens design prevents a photographic lens from giving as nearly perfect definition as would be possible in accordance with the laws of diffraction. These aberrations, entirely unrelated to errors in workmanship, are a result of refraction at a spherical surface. Those of a centered lens system are classified as: (1) Spherical aberration, (2) departure from the sine condition or coma, (3) chromatic aberration, (4) curvature of field and astigmatism, and (5) distortion. The first four affect the defining power of a lens; the fifth, distortion, causes the image to be dissimilar to the object in shape.

1. SPHERICAL ABERRATION

(*a*) DEFINITION.—If rays of monochromatic light, emerging from a single object point situated on the axis of the lens are not refracted through a single axial image point, the lens possesses spherical aberration. (Illustrated in fig. 1.) The amount de-

pends, among other things, upon the shape of the lens—simple lenses of the same powers and apertures, but of different shapes, showing it to greatly different degrees.

A paraxial ray—that is, one very near and parallel to the axis

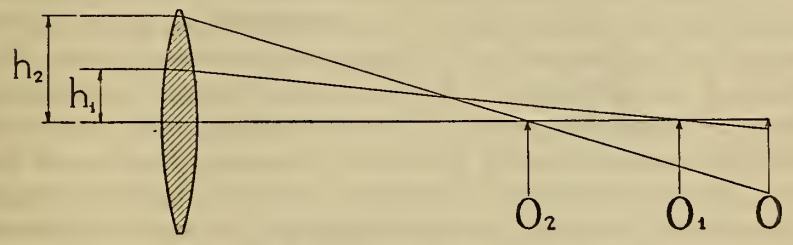

FIG. 1.—*Spherical aberration of a converging lens*

of the lens—is focused at the point O, say, on the axis, while the rays incident at heights h_1 and h_2 are brought to a focus at O_1 and O_2, respectively. The distance $O\ O_2$ is called the longitudinal spherical aberration of the marginal ray and is positive in sign

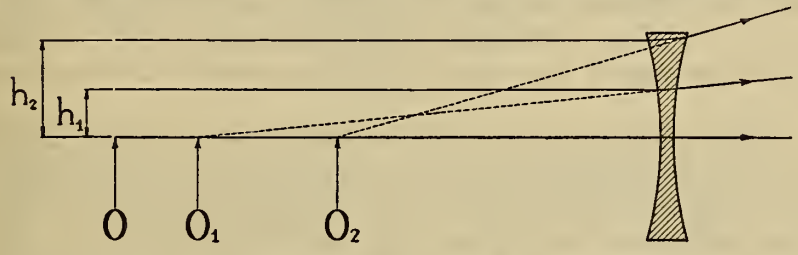

FIG. 2.—*Spherical aberration of a diverging aberration*

when, as in the case shown, O_2 is nearer the real object point than is O. This is the case with all single converging lenses producing real images of real object points.

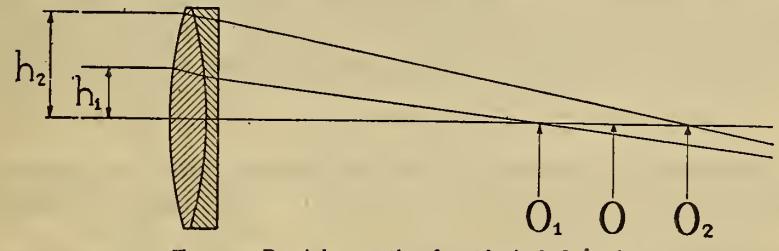

FIG. 3.—*Partial correction for spherical aberration*

The spherical aberration of a single diverging lens is correspondingly always negative, as illustrated in Figure 2.

In a system of two or more lenses it is possible to correct the spherical aberration. For example, as illustrated by Figure 3,

a photographic or telescopic objective is usually *overcorrected* for the marginal ray while the ray incident at about three-quarters of the distance from the center to the edge is *undercorrected.*

(*b*) EFFECT OF SPHERICAL ABERRATION.—Perfect definition requires points of the object to be reproduced as points in the image, but in practice this is impossible for two reasons. By virtue of the diffraction of light a point is imaged as a central disk surrounded by a system of concentric rings, the diameter of which decreases toward a point with increasing aperture of the lens. From combined theoretical and empirical considerations it is recognized that two such imaged points can be distinguished visually when the angle subtended at the center of the lens by the centers of their two diffraction patterns is $\frac{1.22\lambda}{D}$, where λ is the wave length of light and D the diameter of the lens. In practical photographic lens systems the aperture is sufficiently large so that the diffraction pattern of a point is small compared to the circles of confusion arising from the various aberrations; so that diffraction plays a very minor part in determining their resolving power.

There remains much work to be done in evaluating the actual effects of the aberrations alone on the resolving power of a photographic lens, and this becomes a very complicated problem, indeed, when diffraction also enters. K. W. Fritz Kohlrausch [1] has worked out a method for evaluating the spherical aberration of lenses in terms of the deleterious effect on the image, and has applied it to a number of photographic objectives.

For the present we shall inquire only into the general effect of spherical aberration on the image of an axial object point. The diameter of the disk image of a point source of light as affected by spherical aberration is given approximately by the formula, $d=\frac{D\delta}{f}$, where D is the diameter of the zone of the lens for which the aberration is a maximum, f the focal length, and δ the spherical aberration; for example, $O\,O_2$ of Figure 1. The angle subtended by this disk at the rear nodal point of the lens is $\frac{D\delta}{f(f\pm\delta)}$ radians. It might be supposed that two points would not be resolved if their circles of confusion overlap. Inasmuch as the circle of confusion shades off from a bright central nucleus the aberration

[1] K. W. Kohlrausch, "Über die sphärische Korrektion photographischer Objective," aus der Graphischen Lehr-und Versuchanstalt, Wien; 1920.

produces, in general, a haze over the fine detail so that in cases of considerable contrast between the detail and its background resolution may not be entirely lost. Figure 4, for example, shows an enlarged photograph of the images of: (1) A single distant axial point source of light formed by a lens having a large amount of spherical aberration, and (2) the images of two such points whose circles of confusion overlap, but are nevertheless resolved.

As a rule, however, spherical aberration is sufficiently corrected to be of minor importance in affecting the performance of photographic objectives. There appears to be no difficulty in making it distinctly less in magnitude than those other more serious aberrations which are more difficult to correct, owing to the necessity of a photographic lens covering a comparatively large angular field.

2. DEPARTURE FROM THE SINE CONDITION

(*a*) DEFINITION.—The magnification of an image for points near the axis is given by the general equation

$$\frac{n \sin \alpha}{n' \sin \alpha'} = m$$

where α and α' are the angles which the corresponding incident and emergent rays, respectively, make with the optical axis, and n and n' are the refractive indices of the media in which the object and image are respectively located. Since with photographic lenses n and n' are equal, freedom from this aberration requires simply that

$$\frac{\sin \alpha}{\sin \alpha'} = m = \text{constant}$$

for all zones of the lens.

If the object be located at an infinite distance, which practically holds with photographic lenses, except when used for special purposes, as copying, etc., this equation becomes

$$\frac{h}{\sin \alpha'} = \text{constant}$$

where h is the distance of the incident ray from the axis of the lens. Figure 5 illustrates the physical significance of this equation. Two parallel rays of monochromatic light, emerging from an infinitely distant axial object point, focus on the axis at, respectively, O'_1 and O'_2. The point of intersection (N_1 or N_2) of the extensions of the incident and refracted rays being defined as the nodal point of emergence, we have, if the sine condition is ful-

filled, the distances from the nodal point of emergence to the focus $\left(\frac{h}{\sin \alpha'}\right)$ are the same for all zones of the lens. This distance for any given zone being defined as the equivalent focal length of that zone, the condition imposed is that there be no zonal variation in the equivalent focal length.

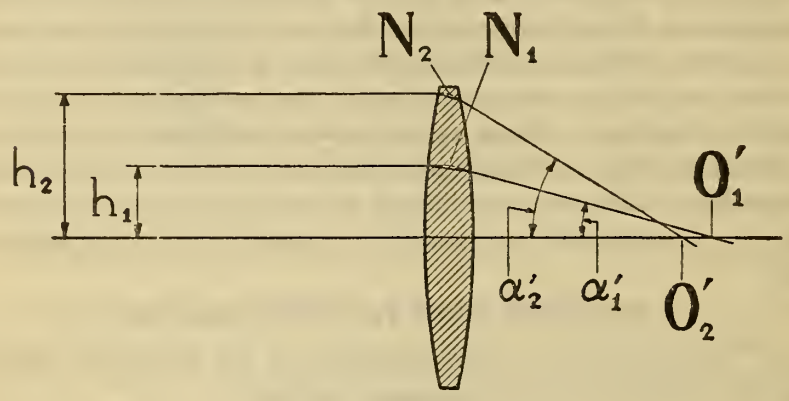

FIG. 5.—*Departure from the sine condition*

(*b*) EFFECT OF DEPARTURE FROM THE SINE CONDITION.—In case the equivalent focal length of any zone of the lens is different from that of another zone the magnifications produced by the two will differ. To illustrate this, consider an object *O B*, Figure 6,

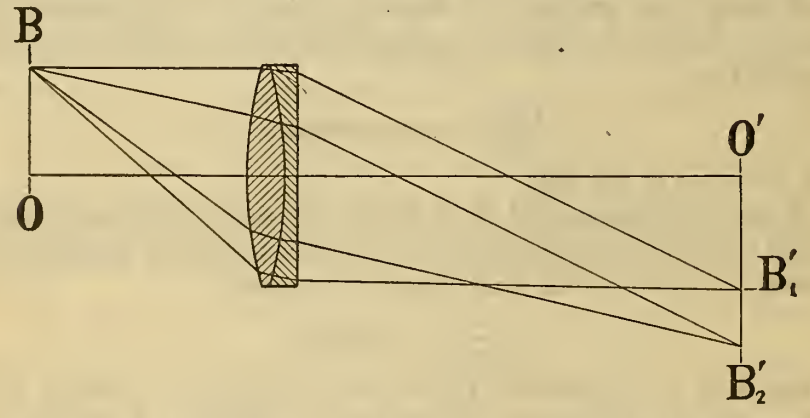

FIG. 6.—*Image from spherical aberration, but with the sine condition not fulfilled*

imaged on the line $O'\ B'_1\ B'_2$. Assuming freedom from spherical aberration, the point *O* on the axis of the lens is imaged as a point at *O'*. Owing to the zonal variation of magnification, however, the object is imaged with a length $O'\ B'_1$ by the outer zone of the lens and with $O'\ B'_2$ by the zone nearer the center of the lens.

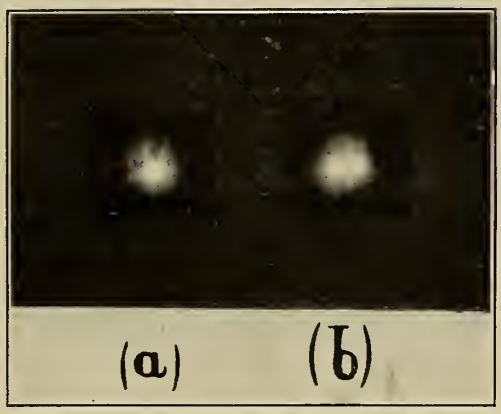

FIG. 4.—*Star images formed by a lens having spherical aberration. Magnification 50 diameters*

(*a*) Single star. (*b*) Double star near limit of resolution

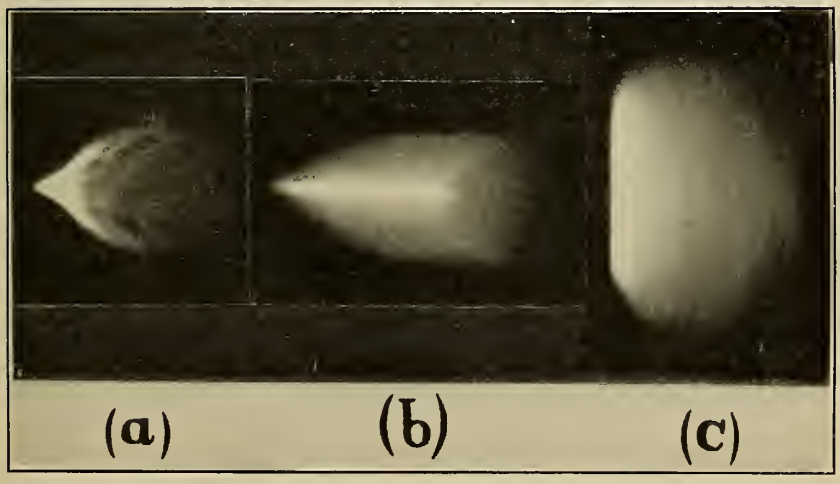

FIG. 7.—*Effect of departure from the sine condition on the images of point and line sources off the axis. The flare is radial to the axis in each case. Magnification 20 diameters*

(*a*) Point source. (*b*) Radial line. (*c*) Tangential line

B'_1 and B'_2 are, however, in the same plane, perpendicular to the axis, since there is assumed to be no spherical aberration present. Thus it results that, although there be freedom from axial spherical aberration, the images formed by the outer zones of the lens are not punctiform but overlapping circles, the diameters of which increase with the diameter of the zone. This is because a pencil of rays refracted by a given zone is in the form of a hollow frustum of a cone, with each small bundle of rays comprising the pencil focusing on the circle at the smaller end of the frustum, called the comatic circle by H. Dennis Taylor.[2] Thus the image at B'_2 should be a circle of smaller diameter than the one at B'_1. As a result of these overlapping circles, a point B off the axis is imaged by the lens as a pear-shaped figure with a small, bright disk farthest from the axis and an enlarged part of diminishing intensity extending toward the axis. Because of the form of this composite image the defect is known as *coma*.

Coma reduces the resolving power through the masking effect of the "tail of the comet." When a lens is undercorrected for coma, as in the present illustration, the flare, being directed toward the axis, does not affect the resolution of points lying farther away from the axis. A circle, for example, about the axis as center would have its outer circumference sharply defined, but the inside edge blurred. Figure 7 shows the appearance of the image of : (*a*) A point source, (*b*) a line in the direction of, and (*c*) the same line perpendicular to this *comatic* flare, formed by a lens having this aberration.

3. CHROMATIC ABERRATION

(*a*) AXIAL.—(1) *Definition.*—When white light is used the component wave lengths are differently refracted, giving rise to variation in the focal length with the color. The failure of a lens free from spherical aberration to reproduce an axial point source of white light as a single axial image point is known as axial chromatic aberration. (Illustrated for a single converging lens by fig. 8.) Because of the prismatic action white light is broken up into its component colors. The red is focused at O'_1; the violet at O'_2, while the yellow, green, and blue focus between O'_1 and O'_2 in the order named. Consistent with spherical aberration a single converging lens is said to have positive chromatic aberration, while that of a single diverging lens is negative, as

[2] A System of Applied Optics, by H. Dennis Taylor, p. 201.

illustrated in Figure 9. Hence an achromatic positive lens may be produced by combining a positive lens of crown with a weaker negative lens of flint, but having equal and opposite chromatic aberration.

(2) *Effect of axial chromatism.*—Owing to chromatic aberration, the image of a luminous point is a disk whose diameter is that of the out-of-focus image for that color whose focus is farthest from

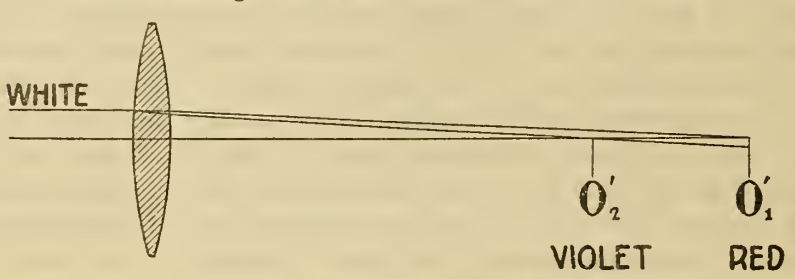

FIG. 8.—*Axial chromatic aberration of a converging lens*

the chosen image plane. Since, however, photographic plates vary greatly in regard to color sensitivity, the effect of chromatism depends to a very large extent upon the plate used, as well as on the lens. If the plate be set at the focus of that color to which it is most sensitive, the nucleus is relatively enhanced and the surrounding disk of lower intensity. This results in a fogging effect somewhat similar to that of spherical aberration, but probably to a lesser degree.

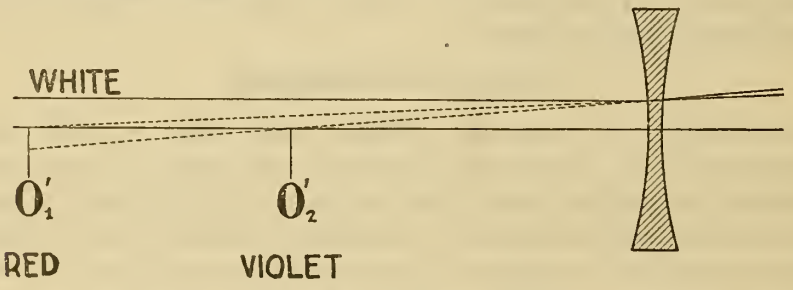

FIG. 9.—*Axial chromatic aberration of a diverging lens*

In fact, the selective action of the plate combined with the use of color filters in conjunction with the lens makes chromatism a minor aberration in rating the performance of photographic objectives.

(*b*) LATERAL CHROMATISM.—(1) *Definition.*—A lens system may be well corrected for chromatic variation in back focal length (axial chromatism) and still be uncorrected for chromatic variation in equivalent focal length, in which case the images of a

nonaxial point for the different colors lie nearly in the same plane, perpendicular to the lens axis, but at different distances from the axis. This latter aberration is known as lateral chromatism. In a lens undercorrected for lateral color, as illustrated by Figure 10, the equivalent focal length for the red being longer than for the violet, the image of a point (B) off the axis is found to show a spectrum with the red end (B'_1) farthest from the axis of the lens and the violet (B'_2) nearest. The opposite occurs with a lens overcorrected for lateral color. Here a point O on the axis is assumed to be imaged at O' by all colors; that is, the lens is free of axial chromatism.

(2) *Effect of lateral chromatism.*—Just as axial chromatism resembles spherical aberration, so does lateral chromatism, as

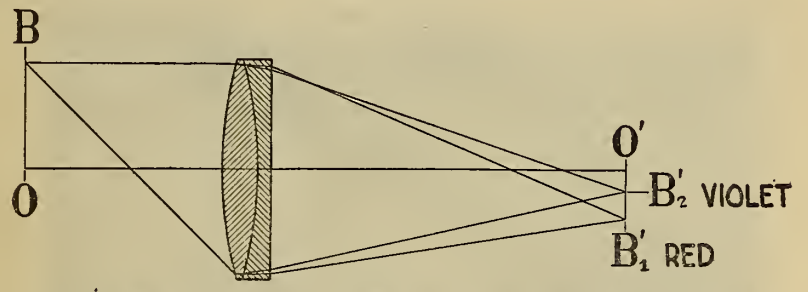

FIG. 10.—*Image free from axial chromatism, but with lateral chromatism present*

indicated in the preceding paragraph, resemble in its effect departure from the sine condition. Furthermore, as with the axial chromatism, the lack of color sensitivity of the ordinary plate and the use of color filters with panchromatic plates greatly reduce the deleterious effect of lateral color. In process work for lithographic purposes, where several pictures of the same size must be made with different colors, it is important, however, that the lens used should be well corrected for lateral color.

4. ASTIGMATISM AND CURVATURE OF FIELD

(*a*) DEFINITION.—When a pencil of rays enters a lens at an angle to the axis, it is focused into two lines at right angles to each other, one (the *secondary*) lying in the plane of the axis, and the other (*primary*) perpendicular thereto. These *focal lines* are separated by a distance called the astigmatic difference, which, measured in the direction of the axis, gives the "astigmatism." Astigmatism occurs only for points off the axis of the lens and, in general, increases with this distance. Because of their limited angular field the effect is not so large as to be serious in telescopic

or even some photographic objectives. In such photographic objectives as the modern anastigmats, the amount of astigmatism is a prime factor in determining the quality of the definition; so the elimination of this aberration becomes one of the most important problems with which the designer has to contend. In fact it is by virtue of the comparatively high degree of correction for this aberration that the anastigmatic type of lens takes its name.

Figure 11 illustrates astigmatism. A_1, A_2, A_3, and A_4 represent the circular cross section of an obliquely emergent pencil of rays (from an object point) converging to the two astigmatic foci f_1 and f_2. The focal line f_2 lies in the meridional plane of the lens

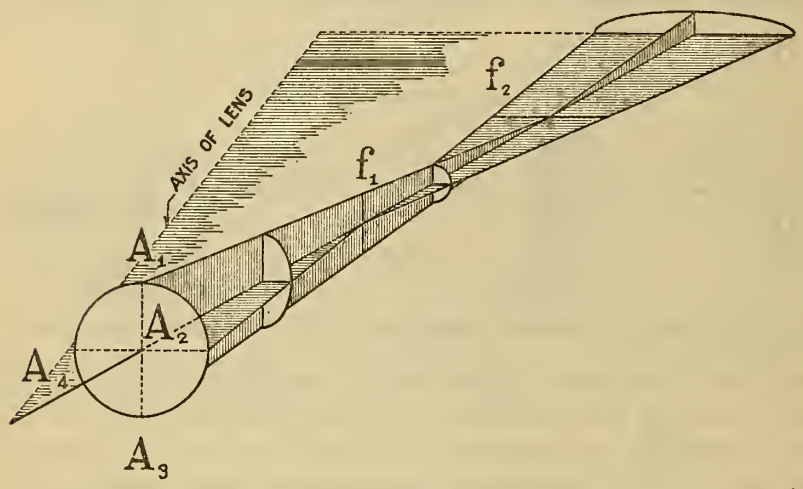

FIG. 11.—*Astigmatism of a small bundle of rays*

and is designated as the secondary focus. The focal line f_1 is perpendicular to f_2 and called the primary focus. They are real line images of an object point. An object consisting of a line parallel to f_1 would be in sharp focus at f_1, the primary focus, while a line parallel to f_2 would likewise focus sharply at f_2, the secondary focus; that is, all lines of the object radial to the optical axis focus at f_2 and all tangential lines (circles concentric with the axis) focus at f_1. At no place along the chief (central) ray of the pencil is there a point focus, the nearest approach to one being nearly midway between the two astigmatic foci, where the image is in the ideal case approximately circular in shape. This disk is called the "circle of least confusion." On both sides of the circle of least confusion the image is elliptical in shape, the major axis of the ellipse being parallel to the nearest focal line. Figure 12 (a)

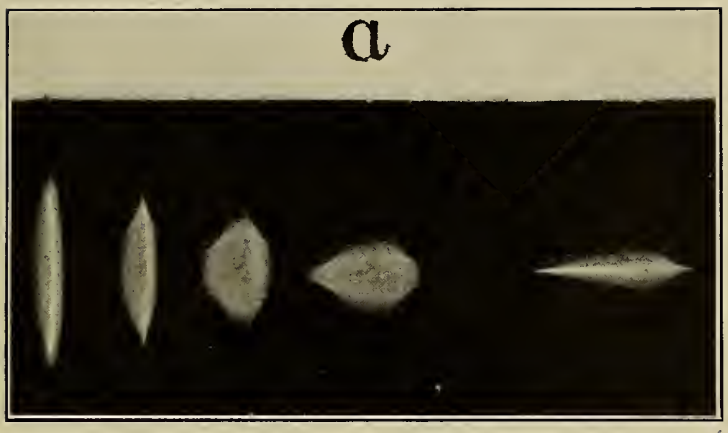

FIG. 12(*a*).—*Successive appearances of the image of a point source along the path between the two astigmatic foci of an oblique pencil of rays with a lens having almost pure astigmatism—primary focus on the left, secondary on the right. It may be noted that the circle of least confusion is not really a circle. Magnification 20 diameters*

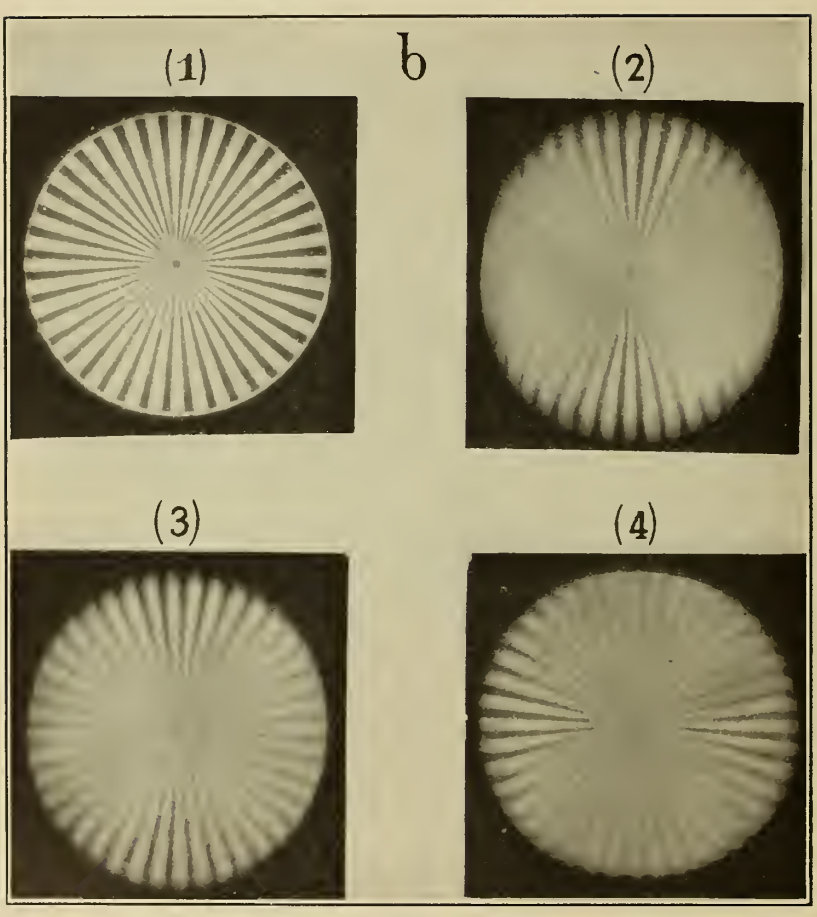

FIG. 12(*b*).—*Test chart. Magnification 50 diameters*

(1) On the axis. (2) Off the axis on the primary image surface, tangential lines in focus. (3) Off the axis near the surface of least confusion. (4) Off the axis on the secondary image surface, radial lines in best focus

illustrates the successive appearances of the image of a point along the path of the chief ray, none of which, however, are a near approach to a circular disk.

In most lenses of the anastigmatic type the astigmatism reaches a maximum value at an angular distance of about 15° from the axis and then decreases to zero at about 22°, beyond which the rate of separation of the focal lines with angular distance is very rapid.

With a single converging lens the surface on which the circles of least confusion lie is cup shaped, having the concave side toward the lens, as illustrated in Figure 13. Here *P* and *S* are, respectively, the primary and secondary astigmatic surfaces and

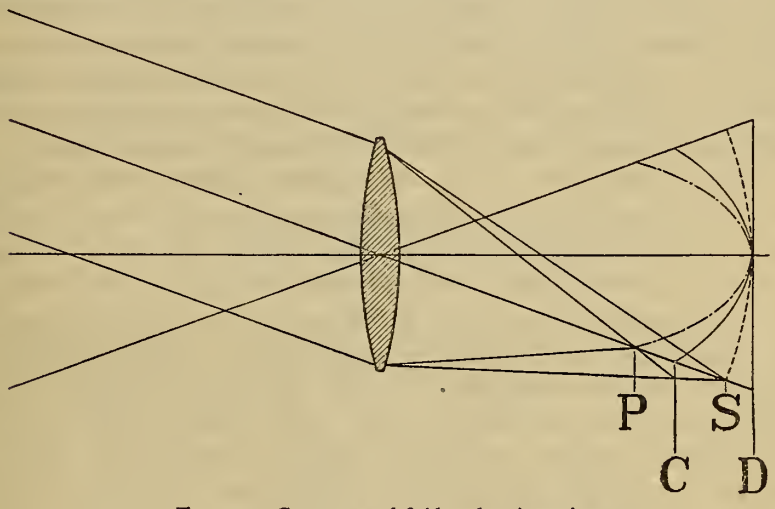

FIG. 13.—*Curvature of field and astigmatism*

Dot dash, primary focus; broken line, secondary focus; full line, surface of least confusion

C the surface of least confusion. The distance from *C* to the plane of the plate, *D*, measured parallel to the axis, gives the departure from flatness of the field.

(*b*) EFFECT OF ASTIGMATISM AND CURVATURE OF FIELD ON DEFINITION.—The effect of astigmatism on the definition of a photographic lens depends upon the position of the plate with respect to the astigmatic foci; that is, it depends on the curvature of field. Consider first a case where the plate cuts all three surfaces. Where it coincides with the primary image surface *P* the image of a point is a short line in the form of an arc of a circle concentric with and perpendicular to the optical axis. If the object at this radius has circles concentric with the axis of the lens, all points on these circles being imaged as lines in the direc-

tion of the arc, the image of the entire circle is not blurred. In this particular case and at this particular part of the plate astigmatism produces no harmful effect. Where the plate coincides with the secondary image surface, *S*, the image of a point is a short line extending radially from the axis. Here radial lines in the object will be clearly defined, their imagery being perfect from the viewpoint of geometrical optics. As a rule, however, the object to be photographed is of such character that it has lines extending in all directions. Under such conditions the parts of the plate in best focus are those which coincide with the *surface of least confusion*, *C*, between the two astigmatic surfaces. These facts are illustrated in Figure 12(b) which gives a photographic reproduction of the appearance of a test chart (1) on the axis, with all lines equally good; (2) in the primary image surface, off the axis, with tangential lines best; (3) near the surface of least confusion, showing best general focus off the axis; and (4) at the secondary image surface, where radial lines are best defined.

It is characteristic of the anastigmatic type of lens that the astigmatic foci do not lie on simple cup-shaped surfaces, but are more or less sinuous in their meridian sections, as will be brought out in the graphs later. For example, the plate may be in its optimum position for central definition and yet the field outside so curved that the astigmatic foci fall on it. Where the surface of least confusion coincides with the plate the definition is, of course, best, but the quality, even here, depends upon the size of the circles of least confusion, which in turn increase with the amount of astigmatism present. On those parts where the primary surface touches the plate, circles concentric about the axis are sharply imaged, while all other lines are blurred; at the secondary surface radial lines are sharp, all others blurred, resulting in a very undesirable streaking of the picture. Thus while with astigmatism present and no curvature of field the definition may be uniformly poor; with astigmatism and curvature both present the image taken as a whole may be still less satisfactory because it is at the same time streaked in parts.

5. DISTORTION

If the four aberrations previously discussed—namely, (*a*) spherical aberration, (*b*) departure from the sine condition (coma), (*c*) chromatic aberration, and (*d*) curvature of field and astigmatism—were all perfectly corrected, a flat object perpendicular to the optical axis of the lens would be imaged with very fine detail

in a single plane perpendicular to the axis. However, the image would not even then be a correct reproduction of the object unless distortion were also corrected. Lenses corrected for distortion are designated orthoscopic or rectilinear. Distortion arises from a variation in the magnification at different distances from the axis of the lens. If the magnification $\left(=\frac{\text{diameter of image}}{\text{diameter of object}}\right)$ increases with distance from the axis the resulting distortion is positive or "pincushion," so-called from the appearance of the image of a network of lines at right angles to each other; while a decreasing magnification gives rise to negative or "barrel" distortion.

For most photographic purposes fine correction for distortion is not of great importance as this defect is likely to be pronounced only near the edges of the plate. Lenses used, however, for such special purposes as process work, architectural photography, and map making must be carefully corrected so that a true scale holds over the whole picture.

III. APPARATUS AND METHODS

1. LENS-BENCH METHODS

Inasmuch as photographic lenses are commonly used with the incident light practically parallel, the object being usually at a large distance compared to the focal length of the lens, parallel rays are used for measuring their characteristics. One method of testing consists in observing through a low-power microscope, and measuring alterations in the image distance by the displacement of the microscope necessary to keep it in focus for the different angular positions of the axis of the lens with the incident parallel rays. A reverse method consists in shifting a fine target of suitable size into the focal plane of the lens, and observing its image through a telescope focused for parallel light. The reverse method has several points in its favor. In the first place a distant target having the vertical and horizontal lines necessary for determining the amount of astigmatism may be somewhat difficult to obtain, while a suitable target to be placed at the focus is readily obtained with ordinary cross lines. Again, the illumination of a distant target is likely to be poor, likewise the atmospheric conditions unsuitable for good "seeing"; whereas a target at the focus may be illuminated in such a manner as to afford maximum precision in making the setting. Furthermore,

J. A. Tomkins [3] has shown that in lens measurements requiring the use of a nodal slide, greater precision in placing the nodal point [4] of the lens over the axis of rotation of the nodal slide is attained when the source of light is at the focus and the emergent parallel rays viewed through a telescope.

Hartmann [5] has described a method for measuring astigmatism, curvature of field, and distortion to which in many respects the method here used is similar. For long focus lenses Hartmann's method would necessarily require something in the way of special apparatus, whereas the method here employed requires only apparatus which is easily obtainable and which at the same time utilizes the advantages found in placing the object at the focal point of the test lens.

(*a*) Curvature of Field, Astigmatism, Distortion, and Axial and Lateral Chromatism.—These were measured by bench methods with the disposition of the apparatus as shown in Figure 14. Light from a tungsten arc (Pointolite) *A* is focused on the cross lines *C* by means of the condenser *B*. At the center of the face of this condenser is placed a disk of black paper sufficiently large that no direct light from the source *A* enters the test lens at *D*. Thus the cross lines (spider web), imaged by diffused light only, act as independent line sources. It was found that when using this system of dark field illumination more accurate settings could be made than when using dark lines against a bright background. These cross lines—one vertical, the other horizontal—are mounted on the micrometer slide of a small comparator, the direction of travel being horizontal and at right angles to the line of the bench. By an improvised control system of cords and pulleys, the micrometer adjustment may be made

[3] J. A. Tomkins, Phil. Mag., 35, p. 21.

[4] Every thick-lens system has two conjugate axial points having the property that if an incident ray passes through the one the emergent ray passes through the other, and, furthermore, both rays are parallel to each other. These points are known as the *nodal points* of the system. By virtue of the fact that when the lens is rotated about its nodal point of emergence no lateral motion of the image occurs, one is enabled to examine the image at any angular distance from the optical axis through a microscope without the necessity of a lateral shift of the microscope. The *nodal slide* is a device upon which the lens may be rotated about a vertical axis passing through the nodal point of the lens. This instrument in its elementary form consists of a slide which may be rotated about a vertical axis and along which the lens may be shifted in the direction of its optical axis, together with a lateral adjustment for placing the optical axis of the lens to intersect the axis of rotation of the slide.

[5] Hartmann, Objectivuntersuchungen, Zeitschr. Instrumentenk., 24, p. 110; 1904. Briefly, Hartmann's method is as follows: The object, consisting of an illuminated vertical slit, is mounted on a graduated horizontal slide perpendicular to the axis of the test lens, which is in turn parallel to the direction of the optical bench along which the lens may be shifted. An astronomical telescope focused for infinity is used for determining when the light emerging from the test lens is parallel; that is, when the slit is at the focal point of the lens. This telescope is mounted on a finely graduated horizontal circle in order to determine the direction of the emergent parallel beam from the test lens when the slit is shifted laterally. Variations in axial distance of image are read from a scale on the optical bench, while distortion is determined from combined readings on the angular scale and the slide which carries the object target.

from the observer's position behind the astronomical telescope E, which has a magnification of about 65 diameters. The test lens is mounted on a nodal slide F provided with an angular scale G of approximately 11 cm diameter and divided into 5° intervals. The bench slide, supporting the nodal slide, may be shifted along the bench by the rod shown in the figure and its position read on the scale H.

(*b*) METHOD OF ADJUSTMENT.—The following adjustments are necessary: (1) The intersection of the cross lines of the reticule C must lie on the axis of the test lens; (2) at the zero position of the angular scale of the nodal slide, the axis of the lens must be parallel to the direction of motion of the lens carriage along the bench; (3) the axis of the telescope must be parallel to the axis of

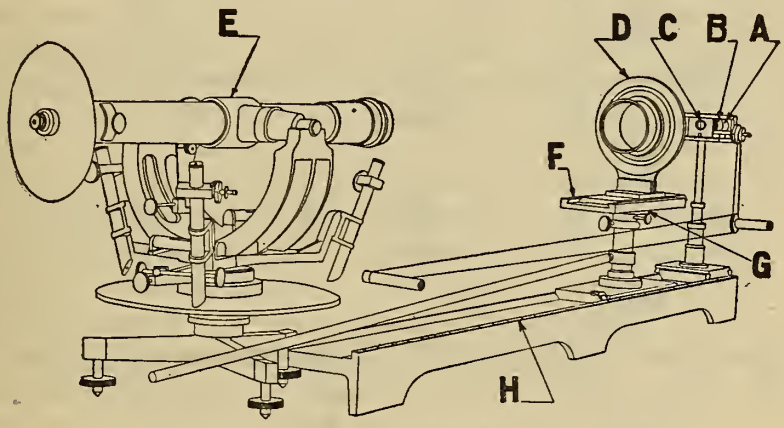

FIG. 14.—*Disposition of apparatus employed in lens bench methods*

the test lens at the zero angle and in approximate coincidence with the latter; and (4) the rear nodal point of the test lens must lie in the axis of rotation of the nodal slide.

To adjust the axis of the test lens parallel to the ways of the optical bench and at the same time coincident with the cross lines, use was made of the fact that all the mirrored images of a point, on the optical axis of a lens, formed by the various surfaces of the lens lie on that axis, hence, in a line of sight with the point. First, then, a reticule with cross lines is placed in the test-lens holder, shown on the nodal slide at S (fig. 15 (a)), so that the point of intersection of the lines is at the point to be subsequently occupied by the center of the lens to be tested. The cross lines are carefully adjusted until their intersection is on the axis of rotation of the nodal slide. To do this they are viewed through the

microscope at *M*, and so located that there is no shift in a direction transverse to the bench when the nodal slide is rotated through 180°. The microscope is left fixed and the nodal slide shifted along the bench toward *O*, as in Figure 15 (b). In the focus of the microscope there is then placed a small mirror, *m*, inclined at 45° to the axis of the microscope, and with a hole in the center. This mirror is displaceable along the ways of the bench and carries a small frosted lamp, *L*, so placed that a light beam is reflected parallel to the axis of the bench. The center of the hole

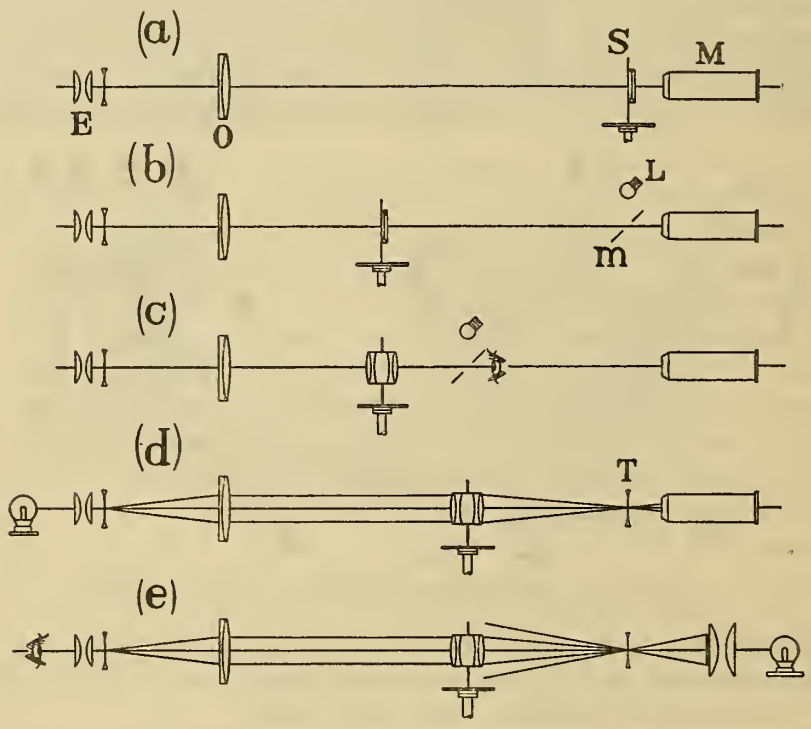

FIG. 15.—*Steps in the adjustment of apparatus for bench method*

in the mirror is adjusted to coincide with the center of the field of the microscope. The line joining the center of the hole with the center of the lens holder lies now on a line which is parallel to the ways of the bench. This line is chosen as the optical axis of the test lens. The mirror-lamp unit is now shifted free of the microscope (as in fig. 15 (c)), and the lens to be tested placed in the lens holder so that a row of small images of the frosted surface of the lamp may be seen reflected from the surfaces of the lens with the eye placed as indicated. By means of leveling screws the lens holder carrying the lens is adjusted and the nodal slide

rotated until the reflected images viewed through the hole in the mirror appear exactly in the line of sight. With this adjustment completed *the lens is located with its axis parallel to the ways of the bench.* Angular positions in the field on either side of the axis of the lens are measured from this setting.

In making the adjustment described, not only are the images from the surfaces of the test lens seen but also those reflected from the telescope objective shown at O, and these serve in like manner for centering the latter on the optical axis of the test lens.[6] This adjustment having been made *the axis of the telescope objective and consequently of the telescope coincides with the axis of the test lens, and both are parallel to the ways of the bench.*

The mirror-lamp unit is thereupon removed and the cross lines (mounted on the micrometer), which serve as test object, are placed in the focus of the microscope with their intersection lying in the center of its field. The telescope focused for infinity is made to serve as a collimator by placing a lamp in front of the eyepiece E to illuminate the cross hairs in its reticule. (Fig. 15 (d)). The test lens is now shifted toward the microscope until the image of this reticule is seen through it. If the nodal point of the test lens is not in the axis of rotation of the nodal slide, a rotation of the lens about this (vertical) axis will cause a horizontal displacement of the image. In this adjustment, then, the lens is moved along the ways of the nodal slide until no such transverse motion is observable. Now, the image of the telescope reticule should coincide with the object cross lines T (fig. 15 (d)), which were previously placed in the focal plane of the microscope with their intersection on the axis of the system. If this is not the case, it means that the ways of the nodal slide were not parallel to the optical axis of the test lens when in its zero position. This is not a serious matter, as the object cross lines T may be made to coincide with the image of the reticule by shifting them laterally and vertically. Now, although the axis of the telescope may not quite coincide with the axis of the test lens, yet it is parallel to the latter and the collimation of the system is retained. In all cases met with in practice this adjustment was very slight. The final adjustment of the nodal point to coincide with the axis of rotation is made by using the illuminated reticule T (fig. 15 (e)) at the focus of the test lens as the object and observing it through the telescope.

[6] The theodolite mounting for the telescope, shown in Figure 14, was found very convenient in making this adjustment, being provided, as it was, with slow motions for adjusting the telescope about the vertical and horizontal axes.

(*c*) Measurement of Curvature of Field and Astigmatism.—If the nodal slide, with the lens properly mounted, is rotated from its zero position (that is, parallel to the bench) through an angle ϕ the lens has a flat field if the distance of the nodal point from the target for emergent parallel rays be $f/\cos\phi$, where f is the equivalent focal length of the lens under test. The initial distance being f, the displacement along the bench to restore the focus is $f/\cos\phi - f$ if the field is flat. If the shift necessary to restore the focus be d, the departure c from a flat field, measured in the direction of the lens axis, and called the curvature, is given by the equation

$$c = f - (f+d)\cos\phi$$

With ϕ larger than about 10° the vertical and horizontal lines of the target are not simultaneously in focus because of the presence of astigmatism. Accordingly, there are, in general, two values of d, d_p giving the amount of displacement of the lens necessary to bring the primary or vertical line again into focus, and d_s the corresponding distance for the secondary or horizontal line.

It is generally desirable to plot the field curves in terms of the focal length of the lens rather than as the actual departure of the image from the plane of the photographic plate set for the best definition at the center. For reducing the departure c to 100 mm equivalent focal length we have, from the simple proportionality of the magnitudes,

$$c_{100} = \frac{f-(f+d)\cos\phi}{f}100$$
$$= 100\,[(1-\cos\phi) - d\cos\phi/f]$$

In making measurements the mean value of d with ϕ measured in opposite directions was taken. A second set of measurements was made on each lens, the lens being newly mounted on the nodal slide for each set. This was done not so much to determine the values of the curvature of the image with more accuracy, but to ascertain if any irregularities occurred in the shape of the field of any lens.

Uncertainty of settings arising from chromatic aberration was eliminated by using a Wratten monochromatic filter, transmitting a wave length of 580 $\mu\mu$, placed between the target and the condenser lens of the illuminating system.

Errors in the measurement of curvature of field and astigmatism.—The errors in the derived results arise from the errors in measuring ϕ and d, and also inaccuracy in placing the nodal point on the axis of rotation. To find the effect on c of an error $\Delta\phi$ we have from $c = f - (f+d)\cos\phi$

$$(\Delta c)_\phi = (f+d)\sin\phi\Delta\phi$$

Experience has shown that $\Delta\phi$ does not exceed 0.00051 radian (1′.75). In the lenses measured ϕ was never greater than 30° and a maximum value of 50 mm for d is fairly representative. Substituting, therefore, these values in the above equation we find

$$(\Delta c)_\phi \not> \pm 0.14 \text{ mm}$$

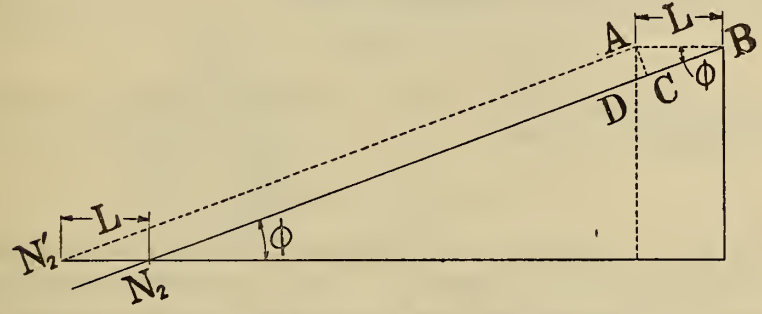

FIG. 16.—*Illustration showing effect of nodal point placed at a slight distance from axis of rotation*

Similarly, the effect of an error Δd is found

$$(\Delta c)_d = -\cos\phi\Delta d$$

With lenses of the aperture ratio and quality of those investigated, the value of Δd at the extreme edge of the field is about ± 0.2 mm. For $\phi = 30°$

$$(\Delta c)_d \not> \pm 0.17 \text{ mm}$$

Another source of error is in placing the nodal point of the lens at the axis of rotation of the nodal slide. Only the displacement in the direction of the ways of the nodal slide rather than the displacement perpendicular thereto is of concern as the latter can be made insignificant by rotating the lens through 180° and adjusting it laterally until the axial image retains its position. Figure 16 illustrates the effect of a displacement, L, of the nodal point, N_2, from the axis of rotation in the direction of the optical axis of the lens. If the lens has a flat field a rotation through an angle ϕ

about the axis on which the nodal point is placed causes the image to lie at B. However, if the nodal point occupies a position at N'_2 distant from N_2 by L, a rotation of the lens through the angle ϕ places the image at A, which is projected on the line of measurement; that is, the original axis of the system, at C. For a determination of the flatness of field under these conditions the target should be placed at D. Thus DC is the error Δd arising from the misplacement of the nodal point.

$$\Delta d = DC = DB - CB$$
$$= \frac{L}{\cos \phi} - L \cos \phi$$

The resulting error in curvature of field

$$(\Delta c)_{N.P.} = -\cos \phi \Delta d = -L \sin^2 \phi$$

L was determined experimentally not to exceed ± 0.05 mm. With ϕ at its largest value, 30°

$$(\Delta c)_{N.P.} \not> \pm 0.012 \text{ mm}$$

The error introduced by an inaccuracy in focusing the observing telescope for infinity, of about ± 0.1 mm, is negligible since if we know the distance of the plane of reference from the test lens we are not concerned with a small variation of this plane from the true focal plane of the lens; that is, if the telescope is focused within this error, the rays emerging from the test lens are sufficiently parallel so that the effect on variations in image distance which we are measuring is of the second order.

Thus the *maximum possible* errors of this method when applied to a lens of 500 mm focal length are

$$(\Delta c)_d \not> \pm 0.17 \text{ mm}$$

$$(\Delta c)_\phi \not> \pm 0.14 \text{ mm}$$

$$(\Delta c)_{N.P.} \not> \pm 0.01 \text{ mm}$$

and, hence, the total maximum possible error is not greater than their sum, ± 0.32 mm. When reduced to 100 mm E. F. L. this error drops to a value not greater than ± 0.07 mm or $\pm 0.0007\ f$. The effect of this error on the size of the image of a point source may be found. The width s of the primary image on the photographic plate bears the same ratio to the distance c_p of the primary

focus from the plate that the diameter of the lens bears to its focal length f; that is, $s = \frac{Dc_p}{f}$. For an f:4.5 anastigmat of 500 mm focal length, and at 30° from the axis, c_p is commonly at least 5 mm. This gives $s = 1.11$ mm. Differentiating the expression for s, $\Delta s = \frac{D}{f}\Delta c_p$, we have since $\Delta c_p \not> \pm 0.32$ mm, ± 0.07 as the possible error in a calculated magnitude 1.11 mm. In so far as its practical importance is concerned, therefore, this error may be neglected.

(*d*) Measurement of Distortion.—Distortion may be readily detected by rotating the test lens about its nodal point (axis of the nodal slide), observing the image of the cross lines in the telescope, and at the same time adjusting the test lens along the

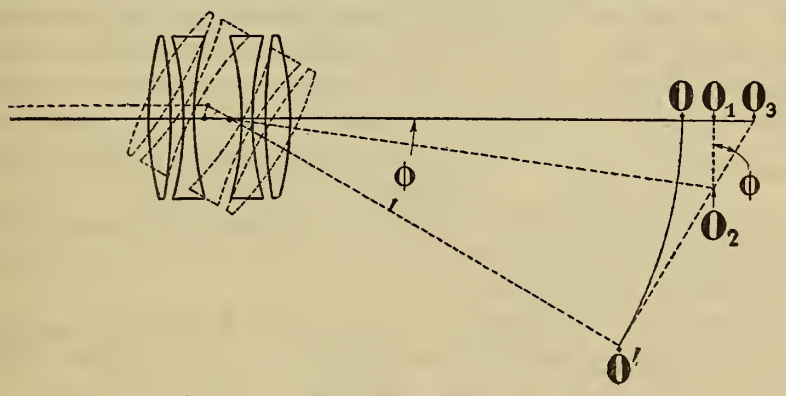

Fig. 17.—*Method of measurement of distortion*

bench for best focus. If for all positions the image falls on the cross lines of the telescope ocular, the lens is free from distortion. Conversely, the lateral displacement of the image with the angular position determines the magnitude of the distortion.

Let O, Figure 17, be the position of the target when the lens is set with its axis parallel to the bench. If there were no distortion rays would still emerge parallel to the bench when the lens is rotated through an angle ϕ about a vertical axis through its nodal point, adjustment having been made for focus in the telescope by moving the target along the bench from O to O_1. Because of the distortion, however, it is found that a transverse motion through a distance $O_1\ O_2$ is necessary in order to keep the original direction of the emergent parallel rays; that is, to bring the image on the cross lines of the telescope ocular.

The lateral displacement $O_1 O_2$ of the object must be measured in the direction of the photographic plate $O' O_3$ since $O_2 O_3$ is the displacement of the image on the plate. We have $O_2 O_3 = O_1 O_2 / \cos \phi$. With the object cross lines mounted on the micrometer screw in the manner already described, the distance $O_1 O_2$ is readily measured for any given value of ϕ and the distortion, which represents the distance from the image of a point to the position which the image would occupy if the lens were perfectly rectilinear, may thus be found.

Errors in measurement of distortion.—In making a setting the lens is rotated about a vertical axis and, hence, the vertical line of the target is used in the setting for coincidence with the cross lines in the ocular of the observing telescope. The result gives the distortion in the primary image plane, but measured parallel to the photographic plate along a line extending radially from the axis of the lens. However, the following consideration shows that the distortion in the primary image surface is practically equal to that in the plane of the plate when set for the focus of the center of the field. $\frac{\text{Distortion in primary image surface}}{\text{Distortion in plane of plate}} = \frac{f \pm c_p}{f}$, where c_p is the *curvature* of the primary image surface, and f the focal length of the lens. Since c_p is only about 1 per cent of f the resultant error is negligible.

The error in measuring the displacement of the image as read from the object micrometer was found to be ± 0.003 mm. This affects the resultant value for distortion, $d = O_1 O_3$, as follows:

$$d = \frac{O_1 O_2}{\cos \phi} = \frac{D}{\cos \phi}$$

$$(\Delta d)_D = \frac{\Delta D}{\cos \phi}$$

$$\gtrdot \frac{\pm 0.003}{\cos 30^\circ} = \pm 0.0034 \text{ mm}$$

An error $\Delta\phi$ in the measurement of the angle ϕ introduces an error

$$(\Delta d)_\phi = D \sec \phi \tan \phi \Delta\phi.$$

Assuming $\phi = 30^\circ$, $D = 0.6$ mm (which is uncommonly large) and 0.00051 radian (1′.75) as the error $\Delta\phi$, gives the negligible value

$$(\Delta d)_\phi \gtrdot \pm 0.0002 \text{ mm}$$

The largest source of error arises from the inaccuracy in placing the nodal point on the axis of rotation of the nodal slide. If the nodal point is distant by an amount, L (fig. 16), from the axis of rotation, a rotation of the nodal slide through an angle ϕ will make necessary a lateral shift of the object in the focal plane by an amount $L \sin \phi$ (in case no distortion is present) to bring the image viewed through the telescope into coincidence with the ocular cross lines. Resolving this lateral displacement of the object cross lines in the direction of the photographic plate, $A\ D$ we find the effect $L \tan \phi$, which for ϕ at its maximum of 30° and $L = \pm 0.05$ mm, becomes ± 0.029 mm. Summing up, the maximum errors in the measurement of distortion of a 500 mm lens at 30° from the axis are:

	mm
Error arising from measurement of lateral displacement of image	±0.0034
Error arising from measurement of angular displacement of lens	± .0002
Error arising from setting of nodal point	± .029
Total maximum error not greater than	±0.0326

When reduced to 100 mm E. F. L. this error becomes ±0.006 mm, which, being only 1 per cent of the maximum distortion of most of the lenses, may be considered a negligible quantity.

(*e*) Measurement of Lateral Color.—The width of the color fringe of an ideal line, arising from lateral chromatism, is found in the same general manner as was distortion. The displacement of the object lines in changing from a wave length of 440 to 700 $\mu\mu$ was measured. Wratten monochromatic filters transmitting practically these wave lengths were placed in turn between the condenser and the target and readings of the micrometer taken when the image in the telescope coincided with the cross lines of the ocular. Hence, the quantity measured is the difference in magnification for light of wave lengths of 440 and 700 $\mu\mu$. To avoid focus adjustments between colors, the test lens was placed for best focus with light of wave length 580 $\mu\mu$. But even with this precaution taken, the image of the cross lines of the target were to a certain extent out of focus, owing to the colored images not lying in the same plane perpendicular to the lens axis. The center of the image being used, however, an appreciable error was not thereby introduced.

Errors in measurement of lateral color.—In this measurement only *difference* in lateral image position is measured; hence, the absolute value of distortion is of no concern. For this reason the inaccuracy of the nodal point setting has practically no

influence, since the error in the measured image position produced thereby is very nearly the same for both colors.

As in the measurement of distortion, $W=\frac{D}{\cos\phi}$ where W is the width of the color fringe measured parallel to the photographic plate; D, the differential lateral shift of the object measured at right angles to the oblique chief ray (maximum value about 2 mm); and ϕ, as before, the angle through which the lens is turned about the nodal point.

$$(\Delta W)_D=\frac{\Delta D}{\cos\phi}$$

and

$$(\Delta W)_\phi = D \sec\phi \tan\phi\Delta\phi$$

$(\Delta W)_D$, the error in measuring the lateral displacement of the target is ± 0.003 mm, the same as in the measurement of distortion, while $\Delta\phi = \pm 0.00051$ radian. For $\phi = 30°$, $(\Delta W)_D \gtrless \pm 0.004$ mm and $(\Delta W)_\phi \gtrless 0.001$ mm, therefore negligible. The above representing the error of a 500 mm lens is when reduced to 100 mm equivalent focal length of the order of ± 0.001 mm.

(*f*) Measurement of Axial Color.—This is observed as the displacement of the lens along the bench necessary to restore the focus, when, with the lens set with its axis parallel to the bench, different filters are placed between the illuminating device and the target. A set of Wratten monochromatic filters transmitting wave lengths of approximately 700, 610, 580, 530, 480, and 440 $\mu\mu$ was used for this purpose. The astronomical telescope is excellently corrected for all the above colors, except the violet at 440 $\mu\mu$, in which case it was found necessary to refocus the telescope for the violet before a setting for this color was taken. For convenience, marks were made on the draw tube of the telescope indicating the proper focus for the violet and yellow, the latter serving satisfactorily for the red, green, and blue. By taking the mean of a series of 10 settings of the lens along the bench for each color, the variation in back focal length for the different colors was found with an error not greater than ± 0.1 mm for a lens of 500 mm E. F. L.

2. MODIFIED HARTMANN METHOD

For measuring spherical aberration and departure from the sine condition, the method originated by Hartmann [7] and extended by Tillyer and Shultz [8] was employed.

In this definite rays of light from a distant axial point source (fig. 18) are isolated by a series of small apertures (in a screen S) diametrically placed in front of the lens to be tested. Consider any ray incident upon the lens at a height h from the axis. After refraction by the lens it intersects the axis at the point O'. The longitudinal spherical aberration is given by the distance between the intersections with the axis of rays incident at various heights. To locate these points the loci a and b of the intersection of the given ray with two planes, both perpendicular to the axis and on

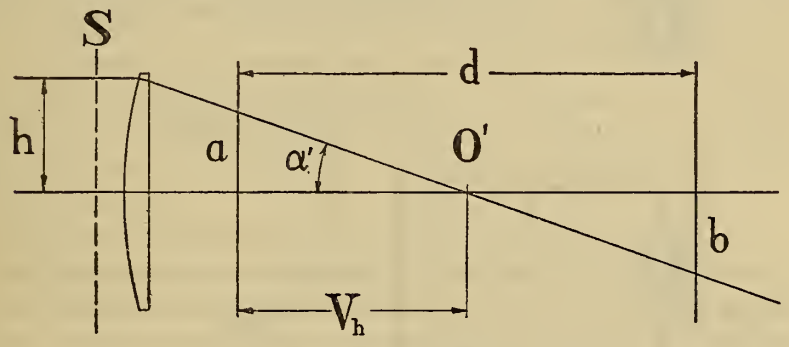

FIG. 18.—*Method employed in measurement of spherical aberration and departure from the sine condition*

opposite sides, respectively, of the focus, are determined. The distance V of O' from the a plane is obtained from the obvious relation $V_h = \frac{a\,d}{a+b}$. From a series of apertures in S we thus get a series of values V_1, V_2, ... By plotting against h the deviation of these values from their mean we have the conventional spherical aberration graph.

In addition to this zonal variation in axial image position, the zonal variation in equivalent focal length (departure from the sine condition) may be derived from the same test. The equivalent focal length for a zone at a height h from the axis is $h/\sin\alpha'$ where α' is the angle which the refracted ray makes with the axis. Since $\tan\alpha' = \frac{a}{V_h}$ and h is the distance of the aperture from the axis, the zonal variations of $h/\sin\alpha'$ may be readily calculated.

[7] Hartmann, loc. cit.
[8] Tillyer and Shultz, B. S. Sci. Paper No. 311.

A diagram of the apparatus is given in Figure 19. To the left, not shown, a 100 c. p. tungsten arc "pointolite" lamp is imaged on a small aperture, of about 1 mm diameter, which constitutes the source. Between the aperture and the source is placed a Wratten and Wainwright monochromatic filter transmitting a narrow band in the region of 580 $\mu\mu$, this wave length being chosen because the lenses investigated were generally used with a *K* filter. On the object side of the test lens and as near as the lens mounting permits is placed the screen with a row of very accurately spaced holes about 1 mm in diameter and 3 mm between centers. This is so adjusted as to isolate rays incident along one diameter of the lens only.

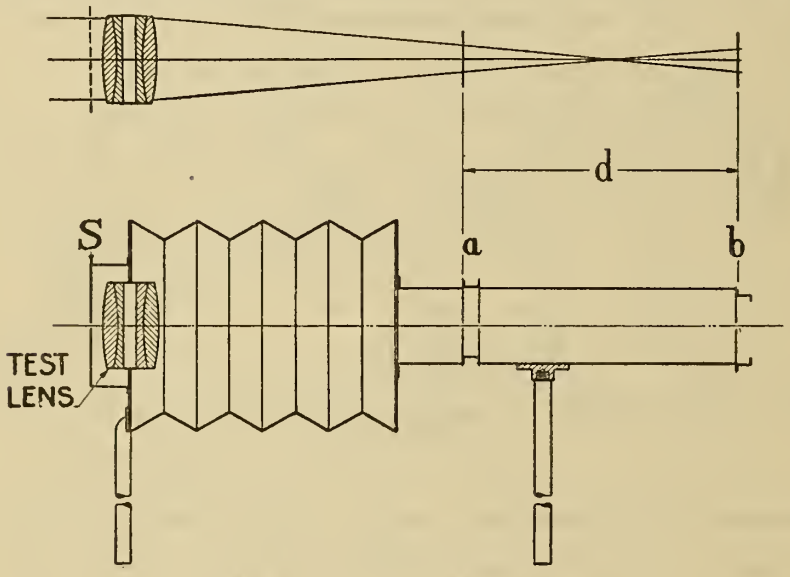

FIG. 19.—*Apparatus employed in adapted Hartmann method*

The axial intersections of the rays fall about halfway between *a* and *b*. Shadowgraphs of the diffraction disks are obtained on the same photographic plate placed first at *a* then at *b*.

The desired accuracy of plate distance was obtained by the following detailed set-up. An Eastman color plate holder, in which springs behind the plate press the emulsion side securely against a metal shoulder, was used. Placed in the cell at *a* or *b*, springs from behind press the plate holder in turn firmly against the side of the cell. A slot in the two faces of the cell *a* permits the light to pass through when exposure is made at the position *b* so that both remain fixed in position during the test. The cell *a* is displaced, as shown, slightly above the optical axis, and

b is lowered with respect to it, thus placing the two exposures side by side on the same plate.

The fixed distance *a b* in the apparatus used, 321 mm, was chosen to give convenient distances between the shadowgraphs for lenses of the focal lengths and aperture ratios dealt with.

To prevent extraneous light passing into the camera through the side entrance of the cell *a*, and fogging the plate in the cell *b*, a "dummy" plate holder consisting of a solid block of wood, of the same size and shape as the regular plate holder, properly slotted to allow the light from the test lens to pass on to *b*, is placed in *a* when an exposure is being made at *b*. Since the camera is entirely inclosed it is not necessary to make the exposures in a dark room, although there should not be any bright objects near the source which might give a set of spurious shadowgraphs.

The following adjustments must be made: (1) The axis of the lens must be mounted perpendicular to the plane of the photographic plate, (2) the central hole in the diaphragm must coincide with the axis of the lens, and (3) the source must lie on the axis of the lens.

The axis of the lens is first adjusted parallel to the bench, on which the apparatus is mounted, by the procedure described under "lens bench methods." Then a plane glass plate is placed in the plate holder and this adjusted, by the reflected images, perpendicular to the optical axis of the test lens. This was easily done since the apparatus was so constructed that the planes of the plates in the positions *a* and *b* were accurately parallel to each other, a setting of the lens axis perpendicular to one plane being sufficient.

The diaphragm on the object side of the lens is adjusted until its central hole, identified by a small slot and hole above it, is in line with the reflections, indicating its coincidence with the axis.

A microscope is now focused on the hole in the mirror and adjusted until the image of the hole is on the cross lines of the microscope ocular. The mirror is removed and the microscope and camera, holding the test lens, are shifted along the bench until the image of the distant point source is seen in focus in the microscope. By shifting the source in vertical and horizontal directions its image may be made to coincide with the cross lines of the microscope. Hence, the source is on the axis of the lens.

It is desirable that the image of the source should be approximately at the center of the tube *a b*. (Fig. 19.) This adjustment is made as follows: The tube length of a low-power microscope may be adjusted to give a working distance of half the distance *a b*. The objective of a microscope so adjusted is placed in contact with the face of the cell *b* and over the narrow slot in this face, and the camera and microscope are moved along the bench, with the test lens kept stationary, until the image of the point source appears in focus in the microscope.

The spacing of the two rows of shadowgraph disks is measured on a small comparator from which the values of a_1, a_2 · · · and b_1, b_2 · · · corresponding to rays whose heights are h_1, h_2 · · · are found. By substituting these respective measurements in the formulas given above, the spherical aberration and departure from the sine condition are determined.

Errors in measuring spherical aberration and departure from the sine condition.—Tillyer and Shultz (loc. cit.) have shown that the errors introduced by a slight tilt of the photographic plate are negligible, as is also the error arising from the measurement of *d*, the distance between the positions *a* and *b*. Defining Δa and Δb as probable errors (which may be either plus or minus in sign), and imposing the practical working conditions, $a=b$ and $|\Delta a| = |\Delta b|$, we may calculate the effect of the probable errors in the measurements of *a* and *b* on the final values of *V* (the distance of the focus from the plane *a*) and *E* (the equivalent focal length of the zone). For this purpose we have:

$$V=\frac{a\,d}{a+b}$$

By the usual method of compounding the errors of a function of two quantities, and substituting $\tan\alpha'$ for $\frac{a+b}{d}$ we have

$$(\overline{\Delta V})^2_{a,b}=\left[\left(\frac{b\Delta a}{a+b}\right)^2+\left(\frac{-a\Delta b}{a+b}\right)^2\right]1/\tan^2\alpha'$$

Since $a=b$ and $|\Delta a| = |\Delta b|$, it follows that

$$(\Delta V)_{a,b}=0.7\,\frac{\Delta a}{\tan\alpha'}$$

Likewise the probable error $(\Delta E)_{a,b}$ may be found. Since

$$E = \frac{h}{\sin \alpha'} = \frac{h\sqrt{(a+b)^2+d^2}}{a+b}$$

$$(\overline{\Delta E})^2_{a,b} = \frac{h^2 \cos^2\alpha'}{(a+b)^2 \tan^2\alpha'}(\overline{\Delta a}^2 + \overline{\Delta b}^2)$$

and similarly

$$(\Delta E)_{a,b} = \frac{0.7\ h \cos \alpha'}{a \tan \alpha'} \Delta a$$

For the f : 4.5 lenses of 500 mm E. F. L. points on the graphs were determined for incident rays whose heights represented aperture ratios of f : 41.7, f : 20.9, f : 13.9, f : 10.4, f : 8.3, f : 7.0, f : 5.2, and f : 4.5. The corresponding values of tan α' were 0.012, 0.024, 0.036, 0.048, 0.060, 0.072, 0.084, 0.096, and 0.108. The value of Δa was found to be 0.001 mm. ΔV, varying inversely as the height of the incident ray, had the following values: ±0.058, ±0.029, ±0.019, ±0.015, ±0.012, ±0.010, ±0.008, ±0.007, and ±0.006 mm, or in terms of the focal length ΔV varied from ±0.00012 f to 0.000012 f.

To find the effect on E of the probable error Δa given above, from Figure 18 we have the obvious relation

$$\frac{a}{d/2} = \frac{h}{f}$$

which by substituting numerical values gives

$$a/160.5 = h/500 \text{ or}$$
$$a = 0.321\ h$$

Substituting this value in the above expression for $(\Delta E)_{a,b}$ we have

$$(\Delta E)_{a,b} = \frac{0.7 \cos \alpha'}{0.321 \tan \alpha'} \Delta a$$

Owing to the small values of α' found with lenses of the aperture ratios used, no appreciable error is introduced by making

$$\cos \alpha' = 1$$

Hence

$$(\Delta E)_{a,b} = 2.2 \frac{\Delta a}{\tan \alpha'}$$

Thus the probable error $(\Delta E)_{a,b}$ is about three times the probable error $(\Delta V)_{a,b}$ and both vary with the height of the incident ray according to the same laws, hence $(\Delta E)_{a,b}$ ranged from ± 0.00036 f to ± 0.000036 f.

An error in measuring the height h of the incident ray affects only E. The screen used to isolate the rays having been carefully calibrated the values of h had a probable error of ± 0.001 mm. Since

$$E = h/\sin \alpha'$$

$$(\Delta E)_h = \frac{\Delta h}{\sin \alpha'}$$

varying from ± 0.00016 f to ± 0.00002 f in the same manner as $(\Delta E)_{a,b}$. Combining the values of $(\Delta E)_{a,b}$ and $(\Delta E)_h$ it is found that

$$0.00039\ f \leqslant (\Delta E)_{a,b,h} \leqslant 0.00004\ f$$

The above permits comparatively large errors in the measurements for rays near the optical axis of the lens, but it happens that we are not much concerned in practice with the exact focus of these rays because of not only the sharpness of the emergent pencil, but also the fact that the illumination of the image contributed by these inner zones is a very small part of the total. Although, therefore, the graphs have been extended to these regions, one should keep in mind that a large amount of error may be present here without detracting greatly from the significance of the results, but such is not the case for zones farther away from the axis. For this reason the aperture ratios of f : 41.7 and f : 20.9 were excluded in determining the mean values of V and E.

IV. RESULTS

1. DESCRIPTION OF GRAPHS (FIGS. 20 TO 52)

(*a*) Curvature of Field and Astigmatism.—The field curves represent a cross section of the image surfaces when cut by a plane containing the axis of the lens. The ordinates represent distance from the lens to the image in terms of the focal length. Thus at the point 1.00 the center of the field is in focus. From these curves the position of the photographic plate for which most of the surface of least confusion will fall on or near the plate may be determined. The abscissas represent angular distances from the optical axis. The entire field may be pictured by rotating these graphs about

the axis of ordinates (axis of the lens). Thus the curve for the surface of least confusion—that is, of the best image in so far as astigmatism is concerned—generates, in general, a saucer-shaped surface either convex or concave toward the lens, or, perhaps, nearly flat over the entire area of the plate which the lens is supposed to cover.

The broken and dotted lines represent, respectively, the primary and secondary astigmatic foci. All object lines extending radially from the axis of the lens focus on the secondary surface, while circles concentric about the axis focus on the primary surface. The surface of least confusion, shown by the solid line, represents, in general, the position of best image.

The astigmatism at any angular distance from the axis is found by measuring the axial distance between the primary and secondary surfaces at that position.

(*b*) Distortion.—The graph for distortion is indicative of increased (positive) or decreased (negative) magnification with distance from the optical axis. The ordinates represent the linear distortion, which is the distance from the actual image of a point to the position of the image which would be produced by a lens (measured in terms of the focal length of the lens) having no distortion. If this curve falls below the axis of abscissas (as in fig. 20), the distortion is negative, the magnification decreasing with distance from the axis.

(*c*) Axial Chromatic Aberration.—The ordinates for axial chromatic aberration represent the wave length in millimicrons; the abscissas, the corresponding image position in terms of the focal length, the average focus between the wave lengths of 440 and 700 $\mu\mu$ being at 1.00.

(*d*) Lateral Chromatic Aberration.—The widths (in terms of the focal length) of the color fringes between wave lengths, 700 and 440 $\mu\mu$, at varying angular distances from the axis are represented by the ordinates. Positive values, indicating that the image for red light lies farthest from the axis of the lens (as in fig. 21), are above the axis of abscissas which represent angular distances from the optical axis.

(*e*) Spherical Aberration and Sine Condition.—Spherical aberration is plotted as the solid line, and correction for sine condition as the dotted. The ordinates give the distance, h, of the incident rays from the axis, measured in terms of the focal length. The abscissas show for spherical aberration the distances of the

images formed by different zones of the lens, 1.00 being the position where the longitudinal aberration on both sides is approximately balanced.

For sine condition the abscissas show the values of $h/\sin \alpha'$ for the corresponding zones of the lens, α' being the angle which the refracted ray makes with the axis.

(*f*) Discussion of Results.—An examination of the graphs shows that, on the scale plotted, individual lenses of the same type and of supposedly the same construction do not give exactly the same performance, and that this variation is more marked with lenses of some manufacturers than with others. It is doubtful if the variation is of enough consequence, however, in the majority of cases, to noticeably affect the value of the lenses when used for ordinary pictorial purposes, but in cases, such as mapping, where extreme definition over the entire area of the plate is desired, slight differences in performance might manifest themselves.

The lenses investigated have been grouped according to their construction in the following manner: Tessar, triplet, four element, air-spaced type, and the adapted tessar type.

(1) *The tessar type.*—The tessar type of lens, whose characteristics are indicated in Figures 20 to 38, inclusive, is, perhaps, the most widely used of the lenses shown. Those included in this work were made by three different manufacturing concerns, designated as manufacturers A, B, and C.[9]

The lenses of manufacturer A show greater variation in the astigmatism present as well as a greater amount of astigmatism (maximum 0.0114 *f*) than do the lenses made by either manufacturers B or C. The best of the A group in this respect (fig. 22) shows nearly the same correction as the poorest made by manufacturers B and C. (Figs. 27 and 33.)

The lens of the A group having the greatest curvature of field (0.0062 *f*) is shown in Figure 21, while that lens having minimum curvature (0.0020 *f*) is nearly as well corrected in this respect as any of the B or C groups.

In regard to spherical aberration the A tessars excel those of the other two makers, the lens having the least spherical aberration, 0.0026 *f* (fig. 25), of any of the tessars tested and an aperture ratio of *f*:4.5; while the one having the greatest amount of

[9] This designation of manufacturers by the letters A, B, C, etc., has significance only for the given type; for example, the A lenses of the tessar type are not by the same manufacturer as the A lenses of the triplet type.

spherical aberration, 0.0049 *f* (fig. 26), and an aperture ratio of *f*:4.5 is superior to many of the lenses of the B or C groups.

Again, the distortion of the A tessars is somewhat higher than that of the others. While that at 10° from the axis is probably negligible for any purpose for which the lens would be used (although in one case (fig. 24) the distortion at this angle is 0.0004 *f*), in this group the rate of increase of distortion with angular distance from the axis is greater than that of the other tessars. It is interesting to note that in all cases but one the distortion of this group of tessars represents the magnification as decreasing with angular distance from the axis of the lens.

The graphs for the aberrations of the B lenses are shown in Figures 27 to 29. These are of more uniform performance than those of either A or C, although allowance should be made for the fact that there were but three lenses of this maker tested.

The B lens showing the maximum astigmatism, 0.008 *f* (fig. 27), is almost as well corrected as the best of the A lenses, and ranks about the same as the poorest of the C lenses. The best astigmatic correction for B lenses gave a value of 0.0054 *f* (fig. 28).

The curvature of field of the B group exceeds that of the A group, the maximum curvature being 0.0066 *f* (fig. 28), while the one having minimum curvature, 0.0035 *f* (fig. 27), is hardly better than the poorest of the C group.

The lenses of the B group having the best correction for spherical aberration, 0.0037 *f* (fig. 27), has, as might be expected, the smallest aperture ratio, *f*:6.4, whereas the other two lenses, whose spherical aberrations amount to 0.0051 *f* and 0.0059 *f*, have aperture ratios of *f*:4.5.

The distortion graphs for the B group show greater consistency than is generally found among individual lenses. In all three cases the distortion at 10° from the optical axis is practically zero and not over 0.0004 *f* at 20° from the axis, a comparatively fine correction for distortion.

Of the nine lenses of the C group, the one having the poorest astigmatic correction, 0.0079 *f* (fig. 33), has about twice the astigmatism of any of the others, 0.0032 *f* (fig. 30).

The tessars having fields most nearly flat are found in this C group (figs. 30, 34, and 36), with a value of 0.0010 *f* as the departure of the surface of least confusion from the plane of the photographic plate.

The spherical aberration of the C lenses ranges from 0.0024 *f* (figs. 31 and 36) to 0.0054 *f* (fig. 38), these having the minimum

and maximum amounts of this aberration, with respective aperture ratios of f:5 and f:4.5.

The distortion graphs for the C lenses, in addition to being quite uniform, show only a small magnitude, in no case exceeding at 10° 0.0002 f—the poorest (fig. 30) having only 0.001 f at 20°.

(2) *The triplet type* (*figs. 39, 40, and 41*).—For making detailed photographs of objects subtending a small angular field the triplet type of lens is the best. By restricting the angular field to only about 20°, it is possible to construct the lens so that excellent performance as regards astigmatism, curvature of field, and distortion is obtained. The other aberrations (spherical, sine condition, and color) are small in proportion to the focal length, hence critical definition is possible.

The triplets tested were made by two manufacturers—A and B. The aberrations of the A lenses are shown in Figures 39 and 40, that of Figure 39 having an aperture ratio of f:7 and the other f:5. The maximum astigmatism of both lenses is nearly the same, 0.0024 f, while the maximum curvature of field is 0.0014 f in the case of the f:7 lens and 0.0032 f with the f:5 lens. The spherical aberration of the f:7 lens is 0.0005 f and of the f:5 lens 0.0018 f. Both of these triplets show only small distortion, that of the f:7 lens being negative and only 0.0001 f at 10° and 0.0003 f at 15° from the axis. The f:5 lens shows positive distortion zero at 10° and 0.0008 f at 20°.

There was only one B triplet. This has a somewhat larger field, as well as a larger amount of astigmatism (0.0048 f) and curvature (0.0070 f) than was found in the two A triplets. The correction for spherical aberration (0.0016 f) is very good. The distortion, amounting to 0.0002 f at 10° and 0.0014 f at 20° from the axis, is larger than that of either of the A triplets.

(3) *The four element, air-spaced type* (*figs. 42 to 51*).—A number of four element, air-spaced types of lenses, with nearly symmetrical construction, were included in this survey. These lenses have apertures varying from f:7 to f:4.5.

As would be expected from a construction nearly symmetrical about the diaphragm, these lenses show good correction for distortion.

Three lenses of this group were made by manufacturer A, one by B, two by C, and three by D.

The A lens of Figure 42 has an aperture of f:7, a useful field of about 20°, and an E. F. L. of 1,245 mm. The astigmatism,

curvature of field, and spherical aberration of this lens are all smaller than in the other two lenses of this group (figs. 43 and 44), which have apertures of f:4.5. The latter lenses, although of like construction, equal aperture, and nearly the same focal length, show appreciably different amounts of aberration. Thus the lens of Figure 43 has 0.0028 f astigmatism, 0.0031 f curvature, and 0.0014 f spherical aberration; while its counterpart of Figure 44 has 0.0042 f astigmatism, 0.0060 f curvature, and 0.0020 f spherical aberration. It appears quite probable that the second lens may have been slightly out of adjustment, as the first was tested immediately after receipt from the factory where it had been readjusted.

The B lens (fig. 45) has nothing out of the ordinary in the way of correction for astigmatism, curvature of field, and distortion. Although the correction for spherical aberration is exceptionally good, the graph for sine condition is very peculiar in appearance as it crosses the axis of ordinates many times. These irregularities are only slightly larger than the probable errors, yet two independent sets of measurements on this lens gave like results. It seems that irregularities in the surfaces would produce irregularities in the graph for spherical aberration as well as for sine condition. It is regretted that this individual lens was not available for further study of its sine condition characteristics.

The two C lenses (figs. 46 and 47), both having aperture ratios of f : 6, show nearly identical performance. The astigmatism, of 0.0064 f in one case and 0.0070 f in the other, compared favorably with that found in the average tessar, although larger than that found in *A* lenses of the four component, air-spaced type. The third lens of this group (fig. 48), with an aperture ratio of f : 4.5, has astigmatism of only 0.0042 f and curvature of field of 0.0015 f, which is smaller than that of the two f : 6 lenses. The spherical aberration of the f : 4.5 lens amounts to 0.0045 f, while the two f : 6 lenses have aberrations of only 0.0030 f. These lenses show excellent corrections for distortion. The lenses show very small amounts of negative distortion out to about 20° from the axis where the distortion changes sign.

The three D lenses show wide variation. The first (fig. 49) has the largest amount of astigmatism, 0.0144 f, of any included in this series of tests, while the second (fig. 51) has astigmatism of only 0.0071 f. On the other hand, the second has about twice the amount of curvature of field as the former. The f : 8 lens of this

group (fig. 50) shows good astigmatic correction, 0.0041 *f*, but the curvature of field is greater than is found in many of the other lenses examined.

(4) *The adapted tessar type.*—The lens shown in Figure 52 is in principle a tessar with the rear component composed of three elements instead of two. This change in construction is presumably the result of either inability of the manufacturer to obtain the correct glass used in the regular tessar type or an attempt to gain better correction by placing more glasses and surfaces at his disposal.

The astigmatism of 0.0046 *f* is small, but the tessar shown in Figure 30 has even less. This lens has greater curvature of field than is found in any of the tessars, with the one exception shown in Figure 21. It has more spherical aberration than is found in any of the same aperture (*f* : 4.5) tessars. The distortion is not especially well corrected, being 0.0002 *f* at 10° and 0.001 *f* at 20° from the axis.

V. SUMMARY AND CONCLUSIONS

The errors or aberrations which affect the performance of a photographic lens system and the characteristic manner in which the lens suffers a loss in definition therefrom are discussed. Methods for measuring the aberrations are described, and graphs showing the aberrations of 33 lenses of the anastigmatic type by different makers are given. Data are thus available for not only the magnitudes of the aberrations of this type of photographic objective, but also for the variations to be found among lenses of like construction by the same maker.

As a result of this investigation no large differences are found between the tessar and the four element, air-spaced lenses. The angular fields covered and the magnitudes of the aberrations are about equal. However, it will be noted from the graphs that the symmetrical construction gives the better correction for distortion. This would appear to indicate the superiority of this type for use in architectural photography or aerial mapping where it is necessary that the reproduction should be true to scale. However, it should be taken into consideration that the tessar, with its cemented rear component, gives no opportunity for flare caused by reflections from these surfaces, and that for the same reason the total percentage of light transmitted by the lens is increased. The increase in speed to be gained therefrom might,

in practice, more than offset the seeming disadvantage of the presence of comparatively large amounts of distortion. Hence, a study of the aberrations is not sufficient in itself to enable one to decide on the general desirability of either type over the other.

The triplet type shows that it may be used in certain cases to better advantages than the others. For obtaining large photographs of single objects at great distances from the camera this lens should prove very valuable. Excellent definition is obtainable by virtue of the good correction for aberrations. Owing to the small angular field and low aperture ratio, this type of lens is probably not equal to the other types where speed combined with a fairly large angular field are of primary importance.

It is well to add here that in a practical rating of photographic lenses the following characteristics should be known: Resolving power as determined photographically; covering power or area of plate covered before the definition becomes too poor; speed, which may vary from that indicated by aperture ratios, owing to poor transmissivity of the glass used or loss by reflections; condition of the lens regarding flare and scattered light; and distortion. With the exception of distortion, it has been considered beyond the scope of this investigation, dealing as it does with aberrations alone, to make measurements of the above quantities. A correlation of the magnitudes of the aberrations with the actual performance of the lens as registered on the photographic plate would undoubtedly be a valuable extension of the present work.

WASHINGTON, April 15, 1924.

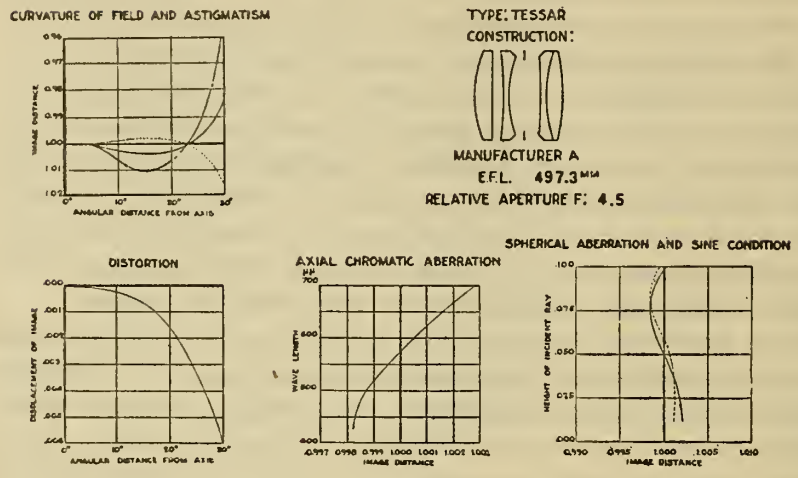
CURVATURE OF FIELD AND ASTIGMATISM
IMAGE DISTANCE
ANGULAR DISTANCE FROM AXIS
TYPE: TESSAR
CONSTRUCTION:
MANUFACTURER A
E.F.L. 497.3 MM
RELATIVE APERTURE F: 4.5
DISTORTION
DISPLACEMENT OF IMAGE
ANGULAR DISTANCE FROM AXIS
AXIAL CHROMATIC ABERRATION
WAVE LENGTH
IMAGE DISTANCE
SPHERICAL ABERRATION AND SINE CONDITION
HEIGHT OF INCIDENT RAY
IMAGE DISTANCE

FIG. 20

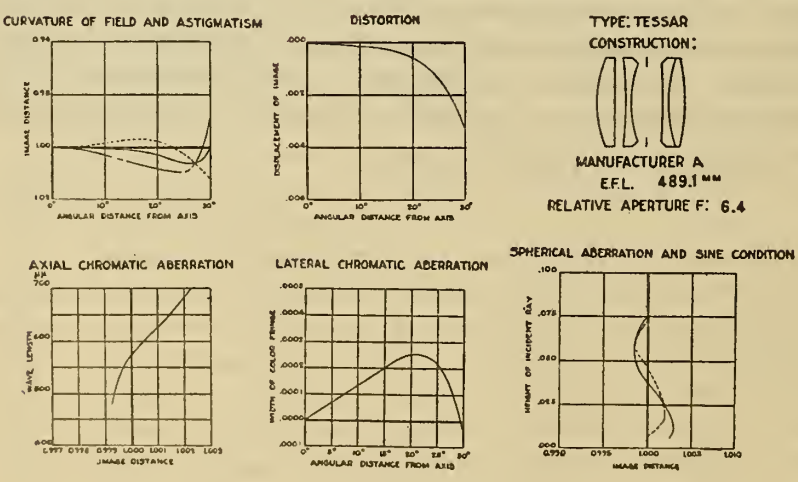
CURVATURE OF FIELD AND ASTIGMATISM
IMAGE DISTANCE
ANGULAR DISTANCE FROM AXIS
DISTORTION
DISPLACEMENT OF IMAGE
ANGULAR DISTANCE FROM AXIS
TYPE: TESSAR
CONSTRUCTION:
MANUFACTURER A
E.F.L. 489.1 MM
RELATIVE APERTURE F: 6.4
AXIAL CHROMATIC ABERRATION
WAVE LENGTH
IMAGE DISTANCE
LATERAL CHROMATIC ABERRATION
WIDTH OF COLOR FRINGE
ANGULAR DISTANCE FROM AXIS
SPHERICAL ABERRATION AND SINE CONDITION
HEIGHT OF INCIDENT RAY
IMAGE DISTANCE

FIG. 21

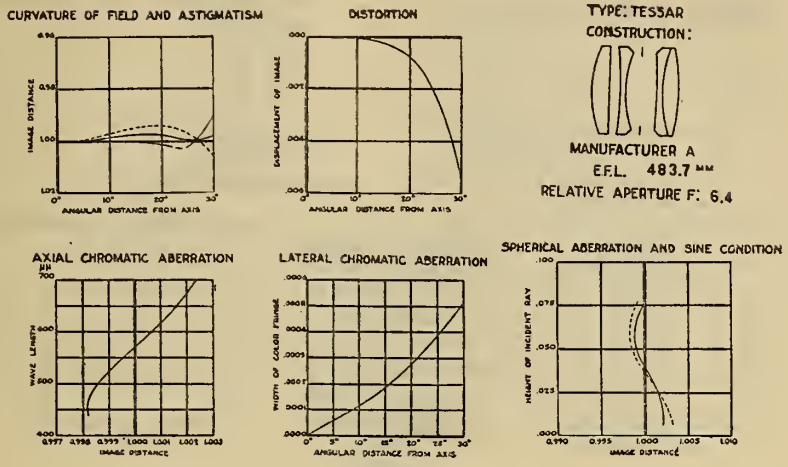
CURVATURE OF FIELD AND ASTIGMATISM
IMAGE DISTANCE
ANGULAR DISTANCE FROM AXIS
DISTORTION
DISPLACEMENT OF IMAGE
ANGULAR DISTANCE FROM AXIS
TYPE: TESSAR
CONSTRUCTION:
MANUFACTURER A
E.F.L. 483.7 MM
RELATIVE APERTURE F: 6.4
AXIAL CHROMATIC ABERRATION
WAVE LENGTH
IMAGE DISTANCE
LATERAL CHROMATIC ABERRATION
WIDTH OF COLOR FRINGE
ANGULAR DISTANCE FROM AXIS
SPHERICAL ABERRATION AND SINE CONDITION
HEIGHT OF INCIDENT RAY
IMAGE DISTANCE

FIG. 22

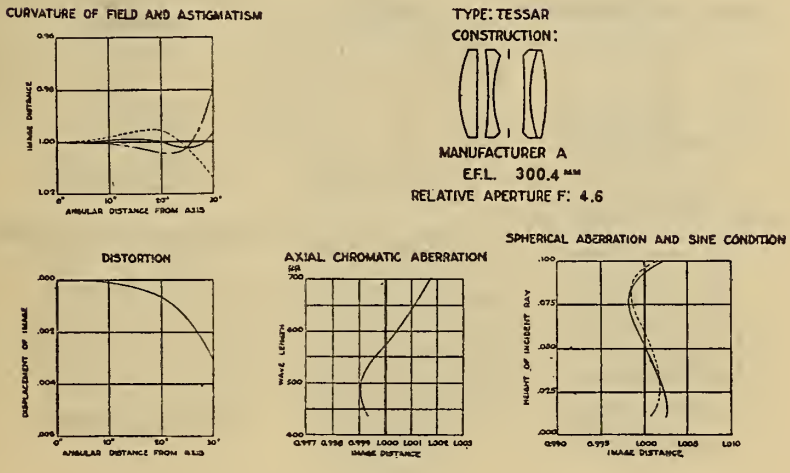
CURVATURE OF FIELD AND ASTIGMATISM
IMAGE DISTANCE
ANGULAR DISTANCE FROM AXIS
TYPE: TESSAR
CONSTRUCTION:
MANUFACTURER A
E.F.L. 300.4 MM
RELATIVE APERTURE F: 4.6
DISTORTION
DISPLACEMENT OF IMAGE
ANGULAR DISTANCE FROM AXIS
AXIAL CHROMATIC ABERRATION
WAVE LENGTH
IMAGE DISTANCE
SPHERICAL ABERRATION AND SINE CONDITION
HEIGHT OF INCIDENT RAY
IMAGE DISTANCE

FIG. 23

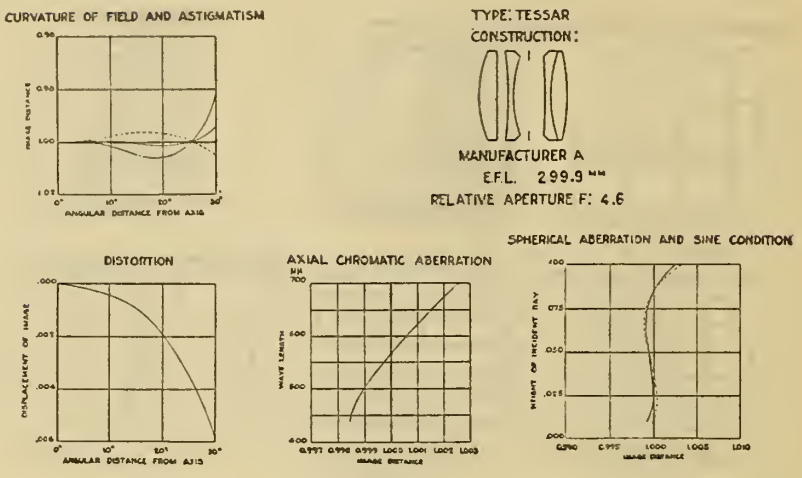
CURVATURE OF FIELD AND ASTIGMATISM
IMAGE DISTANCE
0.96
0.98
1.00
1.02
0°
10°
20°
30°
ANGULAR DISTANCE FROM AXIS
TYPE: TESSAR
CONSTRUCTION:
MANUFACTURER A
E.F.L. 299.9 MM
RELATIVE APERTURE F: 4.6
DISTORTION
DISPLACEMENT OF IMAGE
.000
.002
.004
.006
0°
10°
20°
30°
ANGULAR DISTANCE FROM AXIS
AXIAL CHROMATIC ABERRATION
MM
700
600
500
400
WAVE LENGTH
0.997 0.998 0.999 1.000 1.001 1.002 1.003
IMAGE DISTANCE
SPHERICAL ABERRATION AND SINE CONDITION
HEIGHT OF INCIDENT RAY
.100
.075
.050
.025
.000
0.990 0.995 1.000 1.005 1.010
IMAGE DISTANCE

FIG. 24

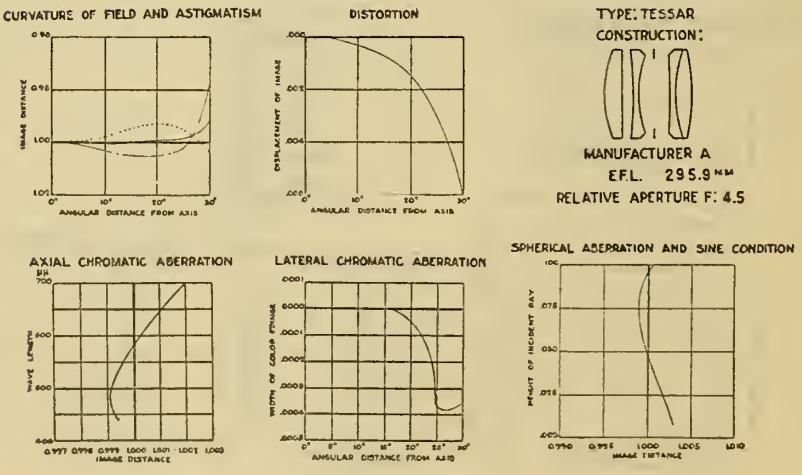
CURVATURE OF FIELD AND ASTIGMATISM
IMAGE DISTANCE
0.96
0.98
1.00
1.02
0°
10°
20°
30°
ANGULAR DISTANCE FROM AXIS
DISTORTION
DISPLACEMENT OF IMAGE
.000
.002
.004
.006
0°
10°
20°
30°
ANGULAR DISTANCE FROM AXIS
TYPE: TESSAR
CONSTRUCTION:
MANUFACTURER A
E.F.L. 295.9 MM
RELATIVE APERTURE F: 4.5
AXIAL CHROMATIC ABERRATION
MM
700
600
500
400
WAVE LENGTH
0.997 0.998 0.999 1.000 1.001 1.002 1.003
IMAGE DISTANCE
LATERAL CHROMATIC ABERRATION
WIDTH OF COLOR FRINGE
.0001
.0002
.0003
.0004
.0005
0°
5°
10°
15°
20°
25°
30°
ANGULAR DISTANCE FROM AXIS
SPHERICAL ABERRATION AND SINE CONDITION
HEIGHT OF INCIDENT RAY
.100
.075
.050
.025
.000
0.990 0.995 1.000 1.005 1.010
IMAGE DISTANCE

FIG. 25

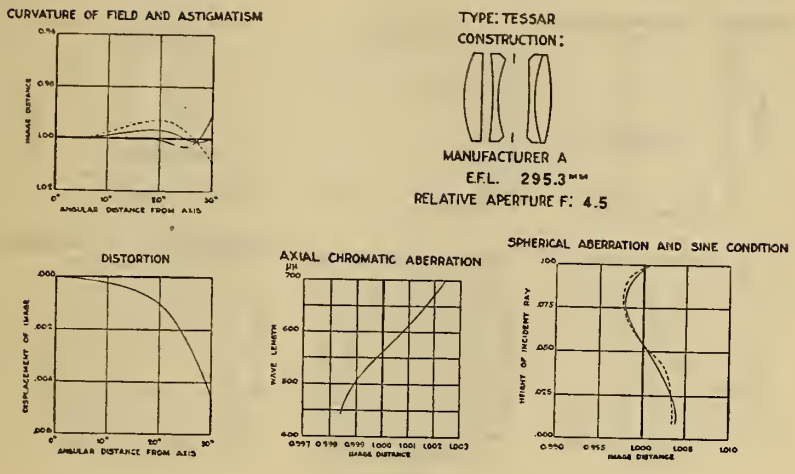
CURVATURE OF FIELD AND ASTIGMATISM
IMAGE DISTANCE
ANGULAR DISTANCE FROM AXIS
TYPE: TESSAR
CONSTRUCTION:
MANUFACTURER A
E.F.L. 295.3 MM
RELATIVE APERTURE F: 4.5
DISTORTION
DISPLACEMENT OF IMAGE
ANGULAR DISTANCE FROM AXIS
AXIAL CHROMATIC ABERRATION
WAVE LENGTH
IMAGE DISTANCE
SPHERICAL ABERRATION AND SINE CONDITION
HEIGHT OF INCIDENT RAY
IMAGE DISTANCE

FIG. 26

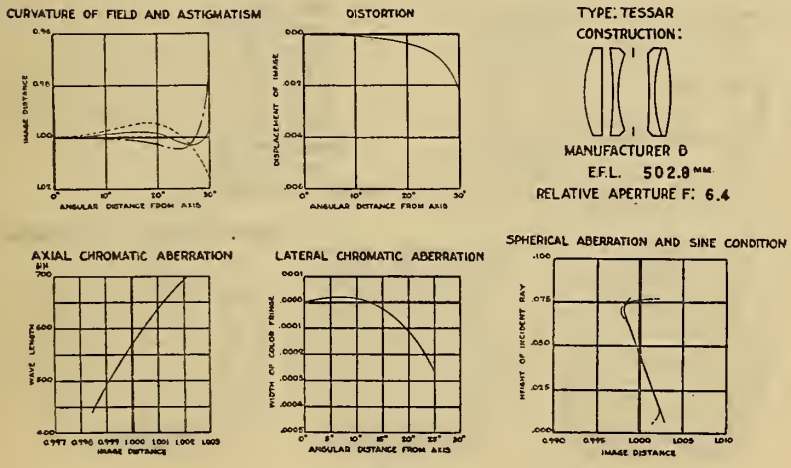
CURVATURE OF FIELD AND ASTIGMATISM
IMAGE DISTANCE
ANGULAR DISTANCE FROM AXIS
DISTORTION
DISPLACEMENT OF IMAGE
ANGULAR DISTANCE FROM AXIS
TYPE: TESSAR
CONSTRUCTION:
MANUFACTURER B
E.F.L. 502.8 MM
RELATIVE APERTURE F: 6.4
AXIAL CHROMATIC ABERRATION
WAVE LENGTH
IMAGE DISTANCE
LATERAL CHROMATIC ABERRATION
WIDTH OF COLOR FRINGE
ANGULAR DISTANCE FROM AXIS
SPHERICAL ABERRATION AND SINE CONDITION
HEIGHT OF INCIDENT RAY
IMAGE DISTANCE

FIG. 27

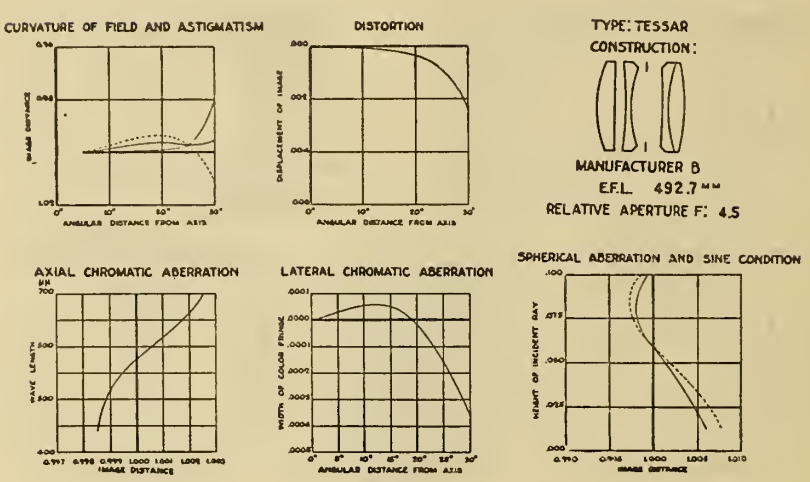
CURVATURE OF FIELD AND ASTIGMATISM
DISTORTION
TYPE: TESSAR
CONSTRUCTION:
MANUFACTURER B
E.F.L. 492.7 MM
RELATIVE APERTURE F: 4.5
AXIAL CHROMATIC ABERRATION
LATERAL CHROMATIC ABERRATION
SPHERICAL ABERRATION AND SINE CONDITION

FIG. 28

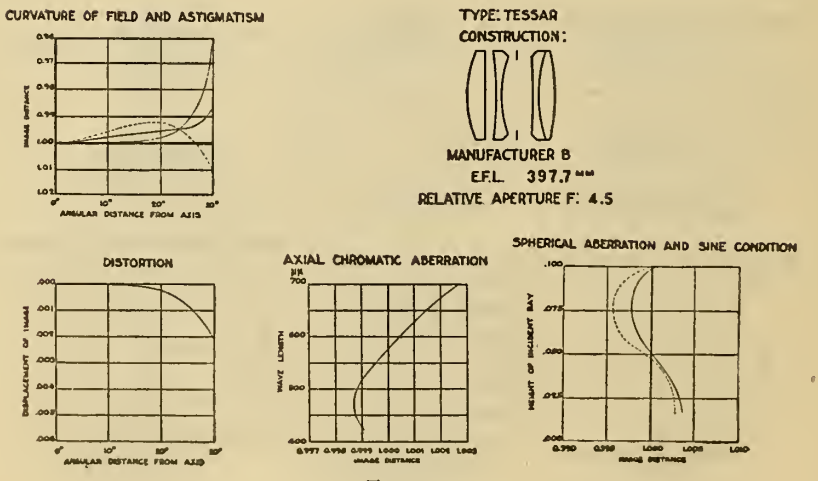
CURVATURE OF FIELD AND ASTIGMATISM
TYPE: TESSAR
CONSTRUCTION:
MANUFACTURER B
E.F.L. 397.7 MM
RELATIVE APERTURE F: 4.5
DISTORTION
AXIAL CHROMATIC ABERRATION
SPHERICAL ABERRATION AND SINE CONDITION

FIG. 29

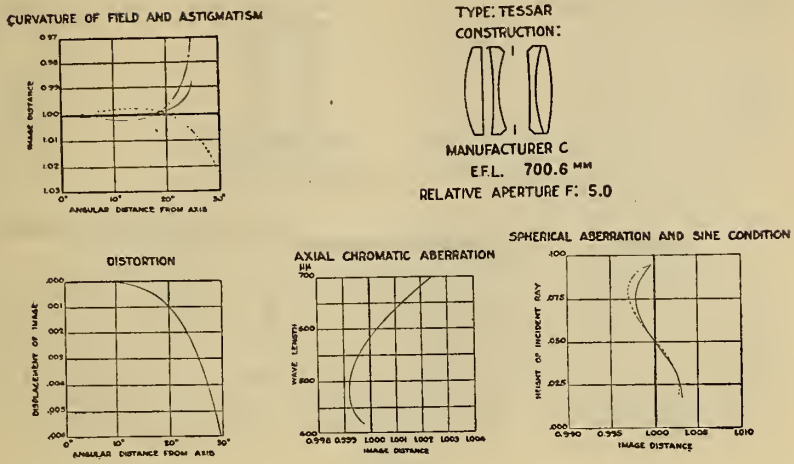
CURVATURE OF FIELD AND ASTIGMATISM
IMAGE DISTANCE
ANGULAR DISTANCE FROM AXIS
TYPE: TESSAR
CONSTRUCTION:
MANUFACTURER C
E.F.L. 700.6 MM
RELATIVE APERTURE F: 5.0
DISTORTION
DISPLACEMENT OF IMAGE
ANGULAR DISTANCE FROM AXIS
AXIAL CHROMATIC ABERRATION
WAVE LENGTH
IMAGE DISTANCE
SPHERICAL ABERRATION AND SINE CONDITION
HEIGHT OF INCIDENT RAY
IMAGE DISTANCE

FIG. 30

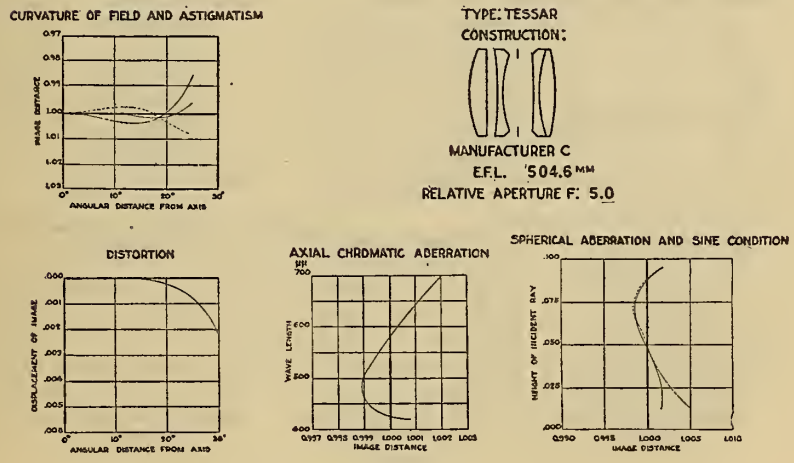
CURVATURE OF FIELD AND ASTIGMATISM
IMAGE DISTANCE
ANGULAR DISTANCE FROM AXIS
TYPE: TESSAR
CONSTRUCTION:
MANUFACTURER C
E.F.L. 504.6 MM
RELATIVE APERTURE F: 5.0
DISTORTION
DISPLACEMENT OF IMAGE
ANGULAR DISTANCE FROM AXIS
AXIAL CHROMATIC ABERRATION
WAVE LENGTH
IMAGE DISTANCE
SPHERICAL ABERRATION AND SINE CONDITION
HEIGHT OF INCIDENT RAY
IMAGE DISTANCE

FIG. 31

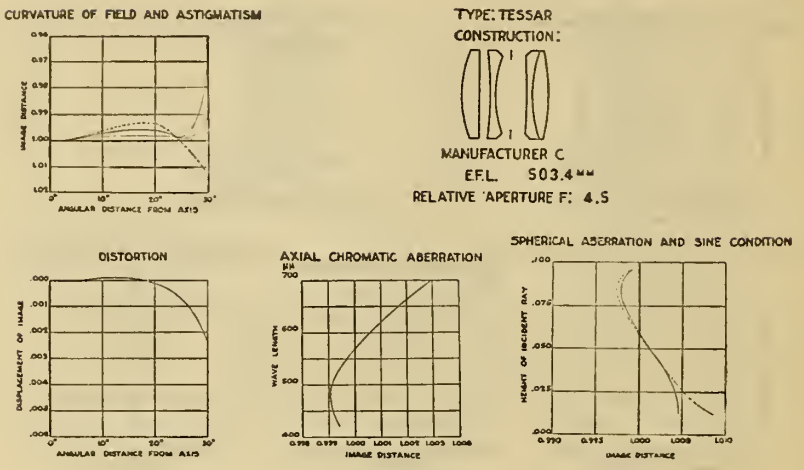
CURVATURE OF FIELD AND ASTIGMATISM
IMAGE DISTANCE
ANGULAR DISTANCE FROM AXIS
TYPE: TESSAR
CONSTRUCTION:
MANUFACTURER C
E.F.L. 503.4 MM
RELATIVE APERTURE F: 4.5
DISTORTION
DISPLACEMENT OF IMAGE
ANGULAR DISTANCE FROM AXIS
AXIAL CHROMATIC ABERRATION
WAVE LENGTH
IMAGE DISTANCE
SPHERICAL ABERRATION AND SINE CONDITION
HEIGHT OF INCIDENT RAY
IMAGE DISTANCE

FIG. 32

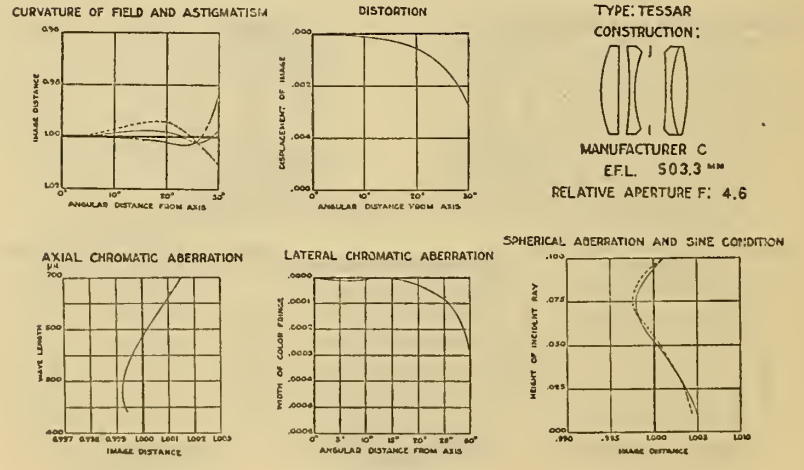
CURVATURE OF FIELD AND ASTIGMATISM
IMAGE DISTANCE
ANGULAR DISTANCE FROM AXIS
DISTORTION
DISPLACEMENT OF IMAGE
ANGULAR DISTANCE FROM AXIS
TYPE: TESSAR
CONSTRUCTION:
MANUFACTURER C
E.F.L. 503.3 MM
RELATIVE APERTURE F: 4.6
AXIAL CHROMATIC ABERRATION
WAVE LENGTH
IMAGE DISTANCE
LATERAL CHROMATIC ABERRATION
WIDTH OF COLOR FRINGE
ANGULAR DISTANCE FROM AXIS
SPHERICAL ABERRATION AND SINE CONDITION
HEIGHT OF INCIDENT RAY
IMAGE DISTANCE

FIG. 33

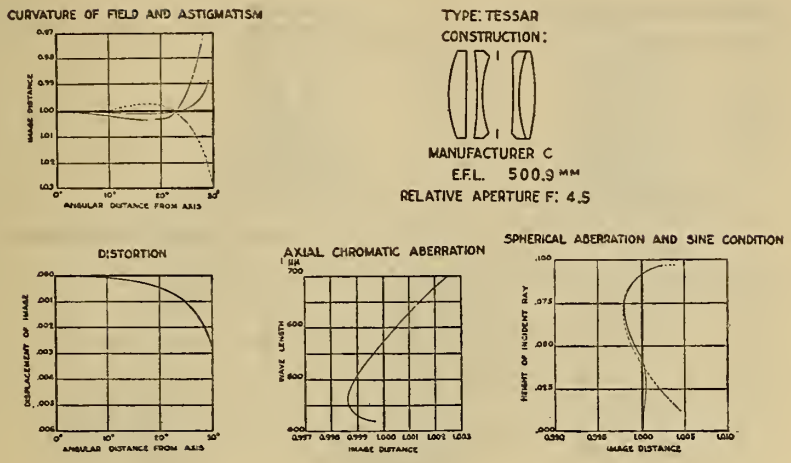
CURVATURE OF FIELD AND ASTIGMATISM
IMAGE DISTANCE
ANGULAR DISTANCE FROM AXIS
TYPE: TESSAR
CONSTRUCTION:
MANUFACTURER C
E.F.L. 500.9 MM
RELATIVE APERTURE F: 4.5
DISTORTION
DISPLACEMENT OF IMAGE
ANGULAR DISTANCE FROM AXIS
AXIAL CHROMATIC ABERRATION
WAVE LENGTH
IMAGE DISTANCE
SPHERICAL ABERRATION AND SINE CONDITION
HEIGHT OF INCIDENT RAY
IMAGE DISTANCE

FIG. 34

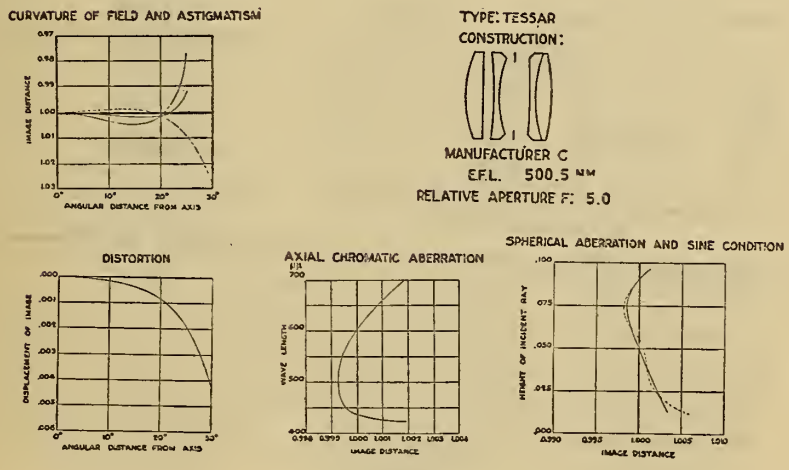
CURVATURE OF FIELD AND ASTIGMATISM
IMAGE DISTANCE
ANGULAR DISTANCE FROM AXIS
TYPE: TESSAR
CONSTRUCTION:
MANUFACTURER C
E.F.L. 500.5 MM
RELATIVE APERTURE F: 5.0
DISTORTION
DISPLACEMENT OF IMAGE
ANGULAR DISTANCE FROM AXIS
AXIAL CHROMATIC ABERRATION
WAVE LENGTH
IMAGE DISTANCE
SPHERICAL ABERRATION AND SINE CONDITION
HEIGHT OF INCIDENT RAY
IMAGE DISTANCE

FIG. 35

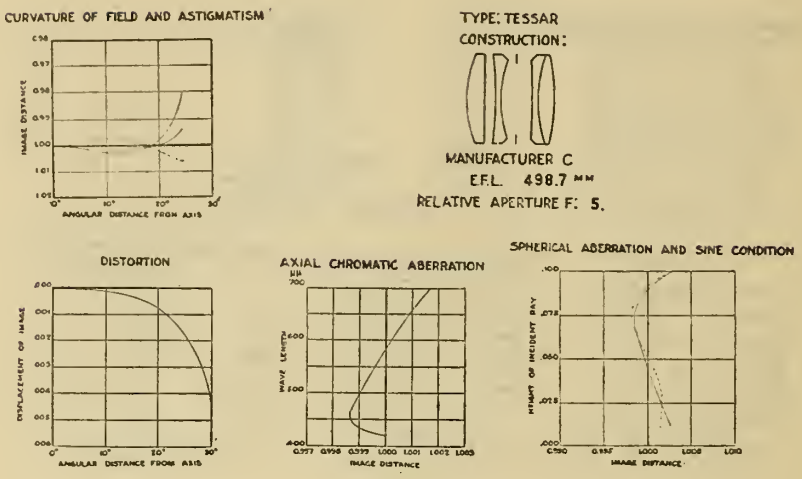
CURVATURE OF FIELD AND ASTIGMATISM
IMAGE DISTANCE
ANGULAR DISTANCE FROM AXIS
TYPE: TESSAR
CONSTRUCTION:
MANUFACTURER C
E.F.L. 498.7 MM
RELATIVE APERTURE F: 5.
DISTORTION
DISPLACEMENT OF IMAGE
ANGULAR DISTANCE FROM AXIS
AXIAL CHROMATIC ABERRATION
WAVE LENGTH
IMAGE DISTANCE
SPHERICAL ABERRATION AND SINE CONDITION
HEIGHT OF INCIDENT RAY
IMAGE DISTANCE

FIG. 36

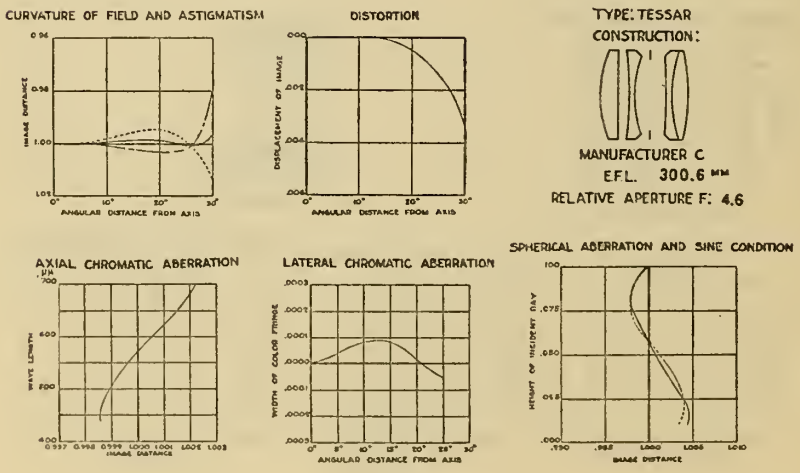
CURVATURE OF FIELD AND ASTIGMATISM
IMAGE DISTANCE
ANGULAR DISTANCE FROM AXIS
DISTORTION
DISPLACEMENT OF IMAGE
ANGULAR DISTANCE FROM AXIS
TYPE: TESSAR
CONSTRUCTION:
MANUFACTURER C
E.F.L. 300.6 MM
RELATIVE APERTURE F: 4.6
AXIAL CHROMATIC ABERRATION
WAVE LENGTH
IMAGE DISTANCE
LATERAL CHROMATIC ABERRATION
WIDTH OF COLOR FRINGE
ANGULAR DISTANCE FROM AXIS
SPHERICAL ABERRATION AND SINE CONDITION
HEIGHT OF INCIDENT RAY
IMAGE DISTANCE

FIG. 37

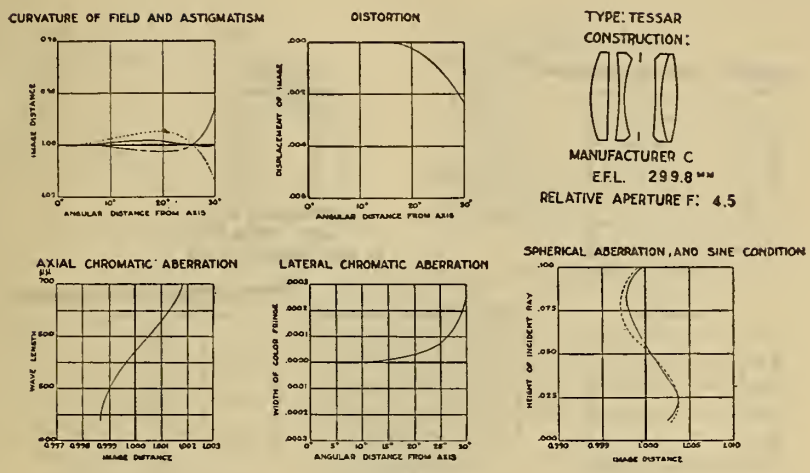
CURVATURE OF FIELD AND ASTIGMATISM
IMAGE DISTANCE
ANGULAR DISTANCE FROM AXIS
DISTORTION
DISPLACEMENT OF IMAGE
ANGULAR DISTANCE FROM AXIS
TYPE: TESSAR
CONSTRUCTION:
MANUFACTURER C
E.F.L. 299.8 MM
RELATIVE APERTURE F: 4.5
AXIAL CHROMATIC ABERRATION
WAVE LENGTH
IMAGE DISTANCE
LATERAL CHROMATIC ABERRATION
WIDTH OF COLOR FRINGE
ANGULAR DISTANCE FROM AXIS
SPHERICAL ABERRATION, AND SINE CONDITION
HEIGHT OF INCIDENT RAY
IMAGE DISTANCE

FIG. 38

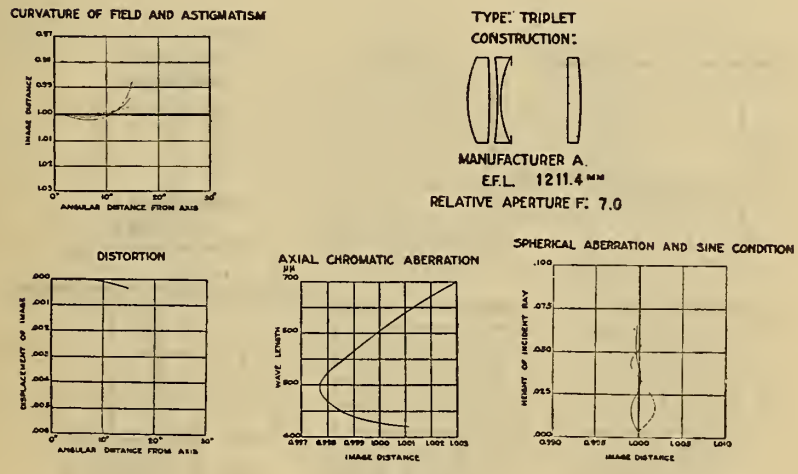
CURVATURE OF FIELD AND ASTIGMATISM
IMAGE DISTANCE
ANGULAR DISTANCE FROM AXIS
TYPE: TRIPLET
CONSTRUCTION:
MANUFACTURER A.
E.F.L. 1211.4 MM
RELATIVE APERTURE F: 7.0
DISTORTION
DISPLACEMENT OF IMAGE
ANGULAR DISTANCE FROM AXIS
AXIAL CHROMATIC ABERRATION
WAVE LENGTH
IMAGE DISTANCE
SPHERICAL ABERRATION AND SINE CONDITION
HEIGHT OF INCIDENT RAY
IMAGE DISTANCE

FIG. 39

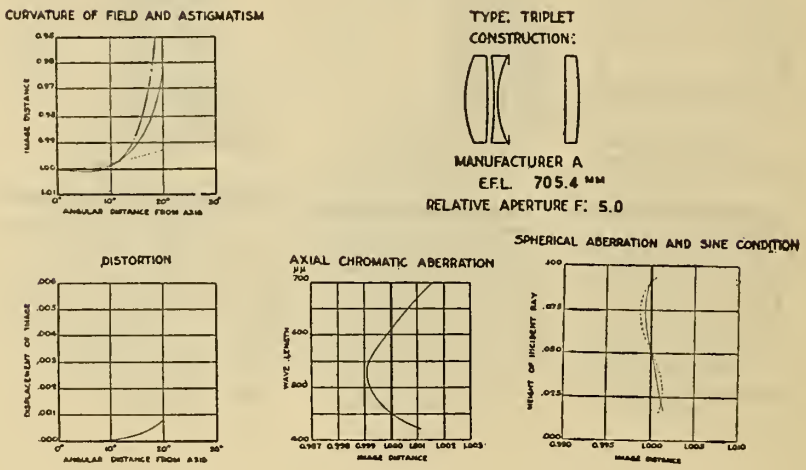
CURVATURE OF FIELD AND ASTIGMATISM
IMAGE DISTANCE
ANGULAR DISTANCE FROM AXIS
TYPE: TRIPLET
CONSTRUCTION:
MANUFACTURER A
E.F.L. 705.4 MM
RELATIVE APERTURE F: 5.0
DISTORTION
DISPLACEMENT OF IMAGE
ANGULAR DISTANCE FROM AXIS
AXIAL CHROMATIC ABERRATION
μμ
WAVE LENGTH
IMAGE DISTANCE
SPHERICAL ABERRATION AND SINE CONDITION
HEIGHT OF INCIDENT RAY
IMAGE DISTANCE

FIG. 40

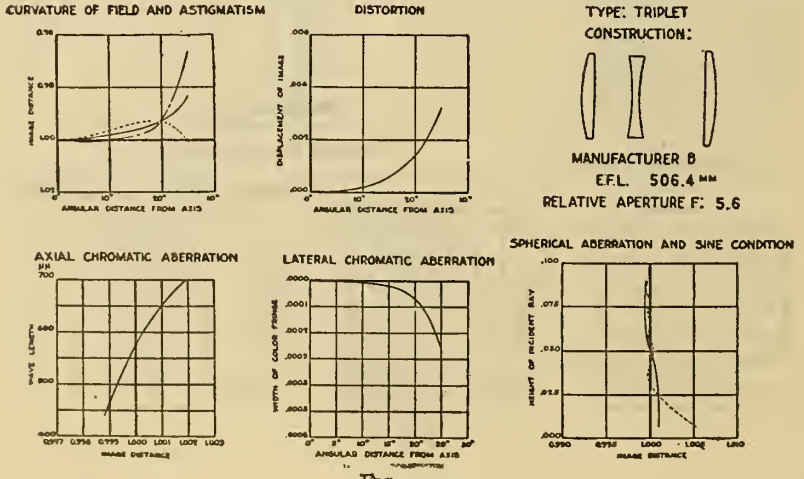
CURVATURE OF FIELD AND ASTIGMATISM
IMAGE DISTANCE
ANGULAR DISTANCE FROM AXIS
DISTORTION
DISPLACEMENT OF IMAGE
ANGULAR DISTANCE FROM AXIS
TYPE: TRIPLET
CONSTRUCTION:
MANUFACTURER B
E.F.L. 506.4 MM
RELATIVE APERTURE F: 5.6
AXIAL CHROMATIC ABERRATION
μμ
WAVE LENGTH
IMAGE DISTANCE
LATERAL CHROMATIC ABERRATION
WIDTH OF COLOR FRINGE
ANGULAR DISTANCE FROM AXIS
SPHERICAL ABERRATION AND SINE CONDITION
HEIGHT OF INCIDENT RAY
IMAGE DISTANCE

FIG. 41

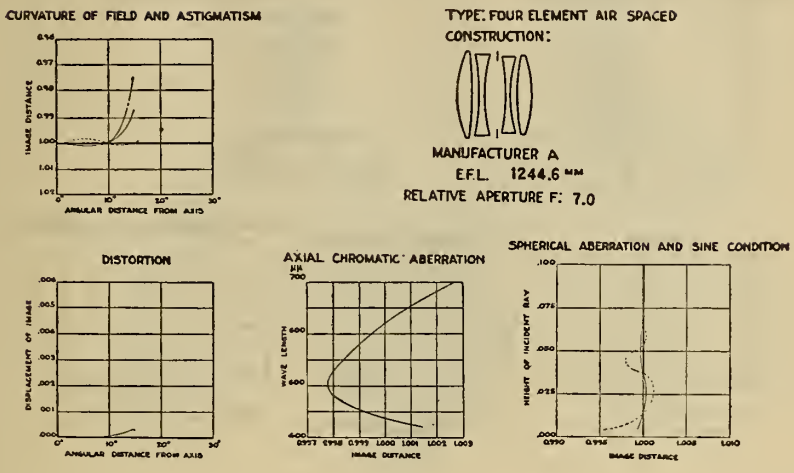
CURVATURE OF FIELD AND ASTIGMATISM
IMAGE DISTANCE
ANGULAR DISTANCE FROM AXIS
TYPE: FOUR ELEMENT AIR SPACED
CONSTRUCTION:
MANUFACTURER A
E.F.L. 1244.6 MM
RELATIVE APERTURE F: 7.0
DISTORTION
DISPLACEMENT OF IMAGE
ANGULAR DISTANCE FROM AXIS
AXIAL CHROMATIC ABERRATION
WAVE LENGTH
IMAGE DISTANCE
SPHERICAL ABERRATION AND SINE CONDITION
HEIGHT OF INCIDENT RAY
IMAGE DISTANCE

FIG. 42

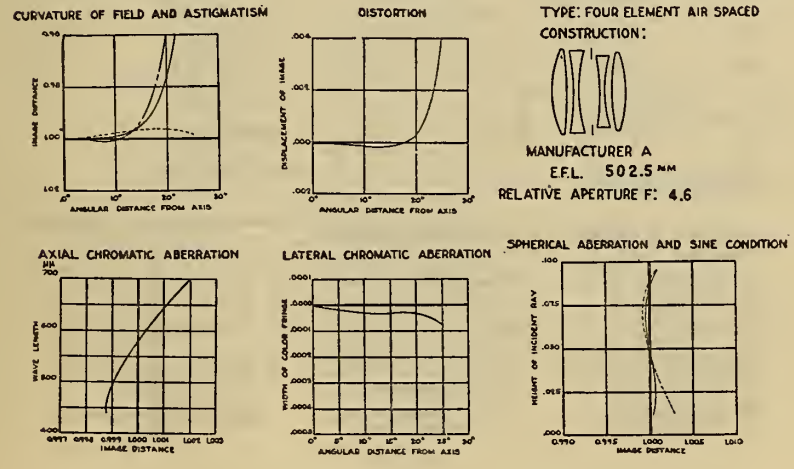
CURVATURE OF FIELD AND ASTIGMATISM
IMAGE DISTANCE
ANGULAR DISTANCE FROM AXIS
DISTORTION
DISPLACEMENT OF IMAGE
ANGULAR DISTANCE FROM AXIS
TYPE: FOUR ELEMENT AIR SPACED
CONSTRUCTION:
MANUFACTURER A
E.F.L. 502.5 MM
RELATIVE APERTURE F: 4.6
AXIAL CHROMATIC ABERRATION
WAVE LENGTH
IMAGE DISTANCE
LATERAL CHROMATIC ABERRATION
WIDTH OF COLOR FRINGE
ANGULAR DISTANCE FROM AXIS
SPHERICAL ABERRATION AND SINE CONDITION
HEIGHT OF INCIDENT RAY
IMAGE DISTANCE

FIG. 43

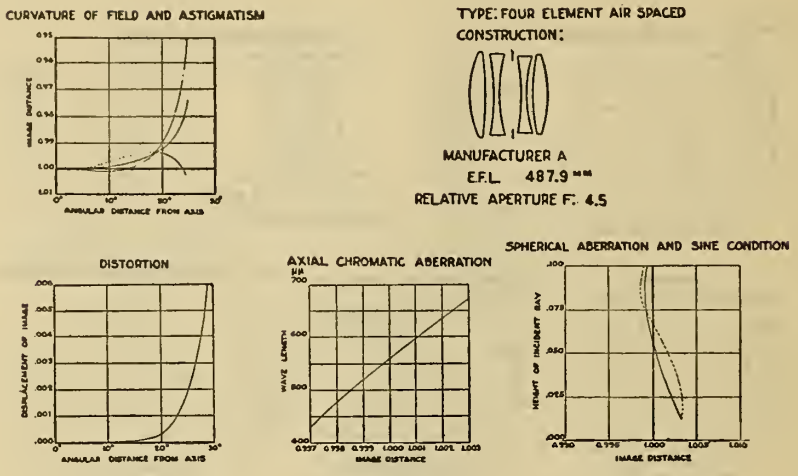
CURVATURE OF FIELD AND ASTIGMATISM
IMAGE DISTANCE
ANGULAR DISTANCE FROM AXIS
TYPE: FOUR ELEMENT AIR SPACED
CONSTRUCTION:
MANUFACTURER A
E.F.L. 487.9 MM
RELATIVE APERTURE F: 4.5
DISTORTION
DISPLACEMENT OF IMAGE
ANGULAR DISTANCE FROM AXIS
AXIAL CHROMATIC ABERRATION
μμ
WAVE LENGTH
IMAGE DISTANCE
SPHERICAL ABERRATION AND SINE CONDITION
HEIGHT OF INCIDENT RAY
IMAGE DISTANCE

FIG. 44

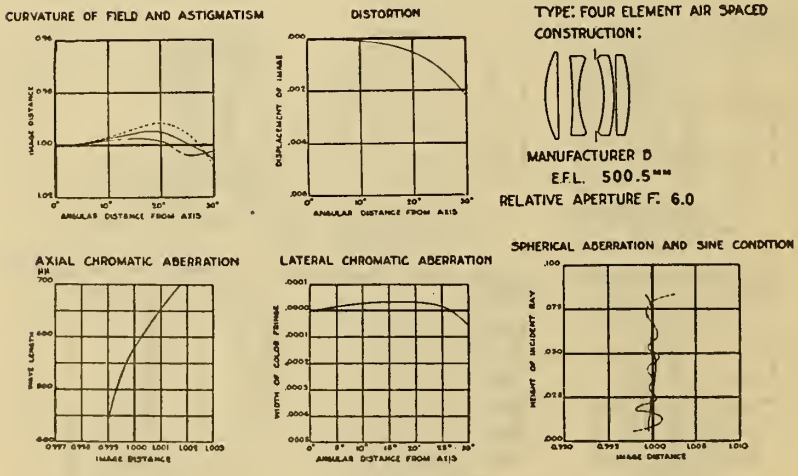
CURVATURE OF FIELD AND ASTIGMATISM
IMAGE DISTANCE
ANGULAR DISTANCE FROM AXIS
DISTORTION
DISPLACEMENT OF IMAGE
ANGULAR DISTANCE FROM AXIS
TYPE: FOUR ELEMENT AIR SPACED
CONSTRUCTION:
MANUFACTURER D
E.F.L. 500.5 MM
RELATIVE APERTURE F: 6.0
AXIAL CHROMATIC ABERRATION
μμ
WAVE LENGTH
IMAGE DISTANCE
LATERAL CHROMATIC ABERRATION
WIDTH OF COLOR FRINGE
ANGULAR DISTANCE FROM AXIS
SPHERICAL ABERRATION AND SINE CONDITION
HEIGHT OF INCIDENT RAY
IMAGE DISTANCE

FIG. 45

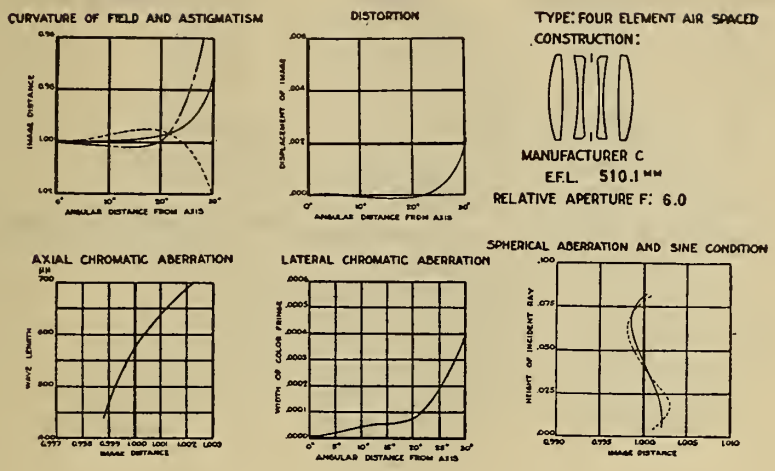
CURVATURE OF FIELD AND ASTIGMATISM
DISTORTION
TYPE: FOUR ELEMENT AIR SPACED
CONSTRUCTION:
MANUFACTURER C
E.F.L. 510.1 MM
RELATIVE APERTURE F: 6.0
AXIAL CHROMATIC ABERRATION
LATERAL CHROMATIC ABERRATION
SPHERICAL ABERRATION AND SINE CONDITION

FIG. 46

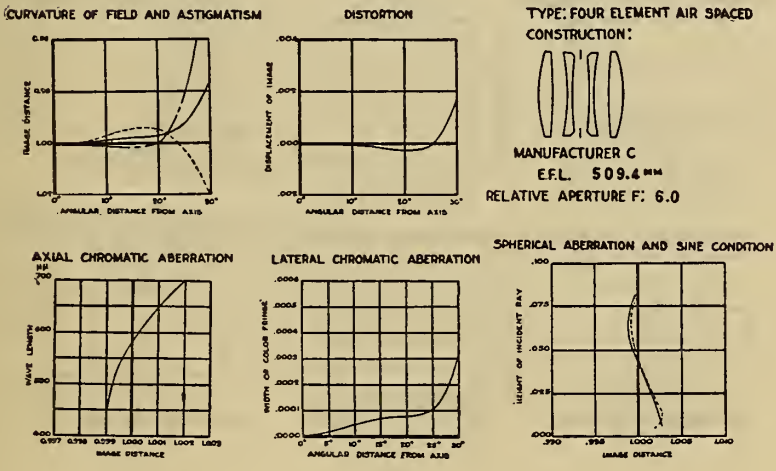
CURVATURE OF FIELD AND ASTIGMATISM
DISTORTION
TYPE: FOUR ELEMENT AIR SPACED
CONSTRUCTION:
MANUFACTURER C
E.F.L. 509.4 MM
RELATIVE APERTURE F: 6.0
AXIAL CHROMATIC ABERRATION
LATERAL CHROMATIC ABERRATION
SPHERICAL ABERRATION AND SINE CONDITION

FIG. 47

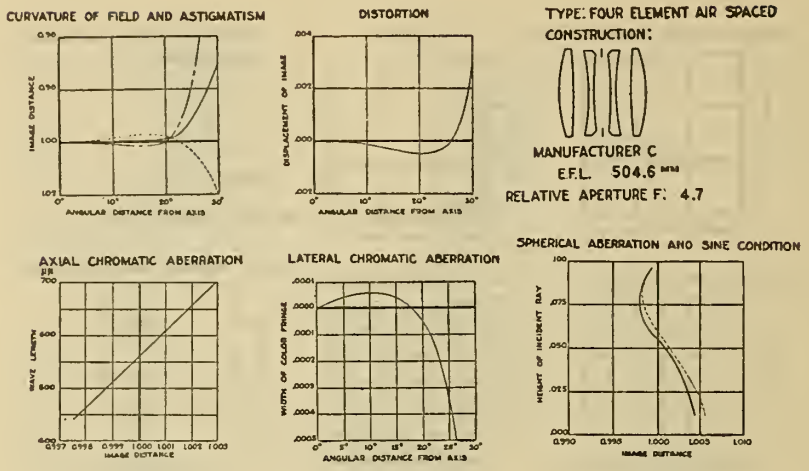
CURVATURE OF FIELD AND ASTIGMATISM
IMAGE DISTANCE
ANGULAR DISTANCE FROM AXIS
DISTORTION
DISPLACEMENT OF IMAGE
ANGULAR DISTANCE FROM AXIS
TYPE: FOUR ELEMENT AIR SPACED CONSTRUCTION:
MANUFACTURER C
E.F.L. 504.6 MM
RELATIVE APERTURE F: 4.7
AXIAL CHROMATIC ABERRATION
WAVE LENGTH
IMAGE DISTANCE
LATERAL CHROMATIC ABERRATION
WIDTH OF COLOR FRINGE
ANGULAR DISTANCE FROM AXIS
SPHERICAL ABERRATION AND SINE CONDITION
HEIGHT OF INCIDENT RAY
IMAGE DISTANCE

FIG. 48

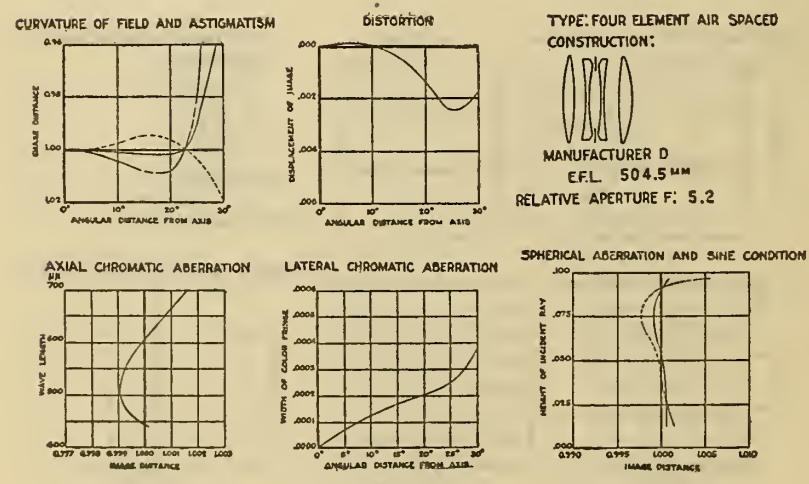
CURVATURE OF FIELD AND ASTIGMATISM
IMAGE DISTANCE
ANGULAR DISTANCE FROM AXIS
DISTORTION
DISPLACEMENT OF IMAGE
ANGULAR DISTANCE FROM AXIS
TYPE: FOUR ELEMENT AIR SPACED CONSTRUCTION:
MANUFACTURER D
E.F.L. 504.5 MM
RELATIVE APERTURE F: 5.2
AXIAL CHROMATIC ABERRATION
WAVE LENGTH
IMAGE DISTANCE
LATERAL CHROMATIC ABERRATION
WIDTH OF COLOR FRINGE
ANGULAR DISTANCE FROM AXIS
SPHERICAL ABERRATION AND SINE CONDITION
HEIGHT OF INCIDENT RAY
IMAGE DISTANCE

FIG. 49

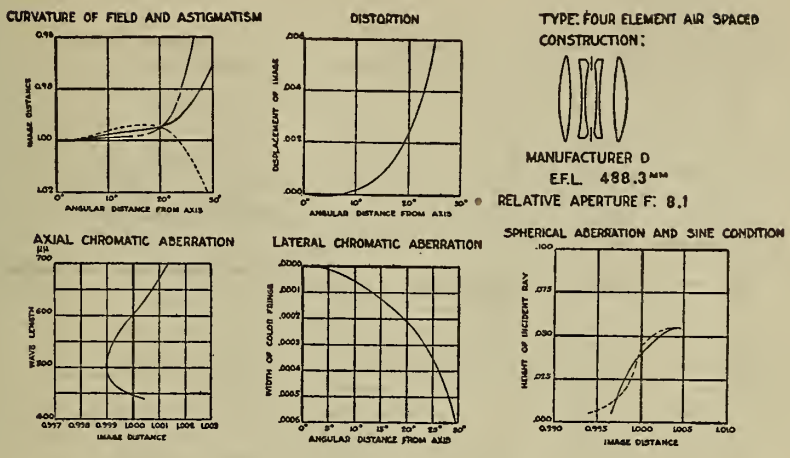
CURVATURE OF FIELD AND ASTIGMATISM
IMAGE DISTANCE
ANGULAR DISTANCE FROM AXIS
DISTORTION
DISPLACEMENT OF IMAGE
ANGULAR DISTANCE FROM AXIS
TYPE: FOUR ELEMENT AIR SPACED CONSTRUCTION:
MANUFACTURER D
E.F.L. 488.3 MM
RELATIVE APERTURE F: 8.1
AXIAL CHROMATIC ABERRATION
μμ
WAVE LENGTH
IMAGE DISTANCE
LATERAL CHROMATIC ABERRATION
WIDTH OF COLOR FRINGE
ANGULAR DISTANCE FROM AXIS
SPHERICAL ABERRATION AND SINE CONDITION
HEIGHT OF INCIDENT RAY
IMAGE DISTANCE

FIG. 50

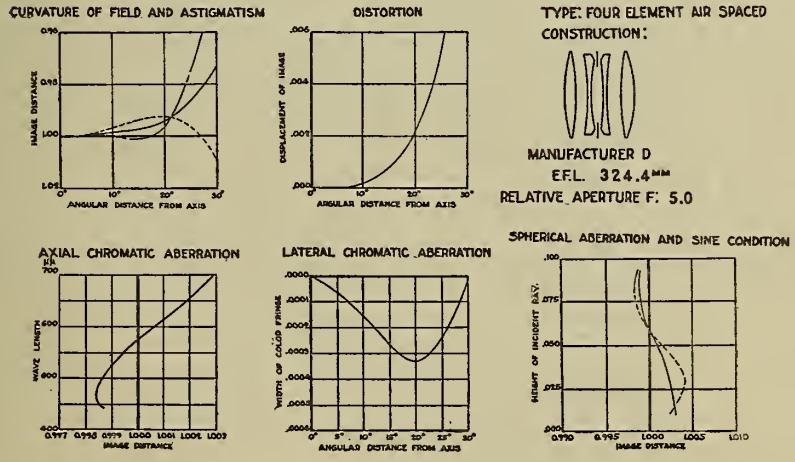
CURVATURE OF FIELD AND ASTIGMATISM
IMAGE DISTANCE
ANGULAR DISTANCE FROM AXIS
DISTORTION
DISPLACEMENT OF IMAGE
ANGULAR DISTANCE FROM AXIS
TYPE: FOUR ELEMENT AIR SPACED CONSTRUCTION:
MANUFACTURER D
E.F.L. 324.4 MM
RELATIVE APERTURE F: 5.0
AXIAL CHROMATIC ABERRATION
μμ
WAVE LENGTH
IMAGE DISTANCE
LATERAL CHROMATIC ABERRATION
WIDTH OF COLOR FRINGE
ANGULAR DISTANCE FROM AXIS
SPHERICAL ABERRATION AND SINE CONDITION
HEIGHT OF INCIDENT RAY
IMAGE DISTANCE

FIG. 51

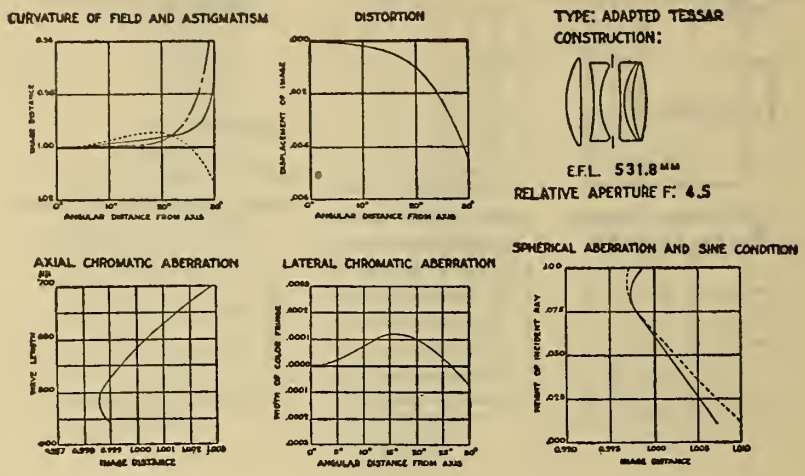
CURVATURE OF FIELD AND ASTIGMATISM
DISTORTION
TYPE: ADAPTED TESSAR
CONSTRUCTION:
E.F.L. 531.8 MM
RELATIVE APERTURE F: 4.5
AXIAL CHROMATIC ABERRATION
LATERAL CHROMATIC ABERRATION
SPHERICAL ABERRATION AND SINE CONDITION

FIG. 52

DEPARTMENT OF COMMERCE
BUREAU OF STANDARDS
George K. Burgess, Director

A RADIOMETRIC INVESTIGATION OF THE GERMICIDAL ACTION OF ULTRA-VIOLET RADIATION

By W. W. Coblentz and H. R. Fulton

SCIENTIFIC PAPERS OF THE BUREAU OF STANDARDS, No. 495